
Morphology, molecules, and character congruence in the phylogeny of South American geophagine cichlids (Perciformes, Labroidei)

HERNÁN LÓPEZ-FERNÁNDEZ, RODNEY L. HONEYCUTT, MELANIE L. J. STIASSNY & KIRK O. WINEMILLER

Accepted: 6 June 2005
doi:10.1111/j.1463-6409.2005.00209.x

López-Fernández, H., Honeycutt, R. L., Stiassny, M. L. J. & Winemiller, K. O. (2005). Morphology, molecules, and character congruence in the phylogeny of South American geophagine cichlids (Perciformes, Labroidei). — *Zoologica Scripta*, 34, 627–651. Phylogenetic relationships among the Neotropical cichlid subfamily Geophaginae were examined using 136 morphological characters and a molecular dataset consisting of six mitochondrial and nuclear genes. Topologies produced by morphological and combined data under parsimony were contrasted, congruence among different partitions was analysed, and potential effects of character incongruence and patterns of geophagine evolution on phylogenetic resolution are discussed. Interaction of morphological and molecular characters in combined analysis produced better resolved and supported topologies than when either was analysed separately. Combined analyses recovered a strongly supported Geophaginae that was closely related to Cichlasomatinae. Within Geophaginae, two sister clades included all geophagine genera. Acarichthyini (*Acarichthys* + *Guianacara*) was sister to the ‘B clade’, which contained the ‘*Geophagus* clade’ (‘*Geophagus*’ *steindachneri* + *Geophagus sensu stricto*, and both sister to *Gymnogeophagus*) as sister to the ‘*Mikrogeophagus* clade’ (*Mikrogeophagus* + ‘*Geophagus*’ *brasiliensis*), and in turn, the *Geophagus* and *Mikrogeophagus* clades were sister to the crenicarine clade (*Crenicara* + *Dicrossus*) and *Biotodoma*. The second geophagine clade included the ‘*Satanoperca* clade’ (*Satanoperca* + *Apistogramma* and *Taeniacara*) as sister to the ‘*Crenicichla* clade’ (*Crenicichla* + *Biotocetus*). Several lineages were supported by unique morphological synapomorphies: the Geophaginae + Cichlasomatinae (5 synapomorphies), Geophaginae (1), *Crenicichla* clade (3), crenicarine clade (1), the sister relationship of *Apistogramma* and *Taeniacara* (4) and of *Geophagus sensu stricto* and ‘*Geophagus*’ *steindachneri* (1), and the cichlasomine tribe Heroini (1). Incorporation of *Crenicichla* in Geophaginae reconciles formerly contradictory hypotheses based on morphological and molecular data, and makes the subfamily the most diverse and ecologically versatile clade of cichlids outside the African great lakes. Results of this study support the hypothesis that morphological differentiation of geophagine lineages occurred rapidly as part of an adaptive radiation.

Hernán López-Fernández, Section of Ecology, Evolutionary Biology and Systematics, Department of Wildlife and Fisheries Sciences, Texas A&M University, College Station, TX 77843–2258, USA. Current address: Section of Integrative Biology, The University of Texas at Austin, Austin, Texas 78712, USA. E-mail: hlopez_fernandez@mail.utexas.edu

Rodney L. Honeycutt, Section of Ecology, Evolutionary Biology and Systematics, Department of Wildlife and Fisheries Sciences, Texas A&M University, College Station, TX 77843–2258. E-mail: rhoneycutt@tamu.edu

Melanie L. J. Stiassny, Department of Ichthyology, American Museum of Natural History, Central Park West at 79th street, New York, New York 10024, USA. E-mail: mljs@amnh.org

Kirk O. Winemiller, Section of Ecology, Evolutionary Biology and Systematics, Department of Wildlife and Fisheries Sciences, Texas A&M University, College Station, TX 77843–2258, USA. E-mail: K-winemiler@tamu.edu

Introduction

Phylogenetic studies of cichlids have traditionally focused on higher-level relationships within the family Cichlidae, and have been generally based on morphological characters (e.g.

Cichocki 1976; Stiassny 1981, 1987, 1991; Oliver 1984; Kullander 1998). However, limited morphological variation and convergence among cichlid taxa result in extensive homoplasy and decreased phylogenetic resolution (e.g. Stiassny 1987,

1991). Morphological convergence is rampant among cichlids probably due to the enormous ecological versatility of the group, which has undergone frequent adaptive modifications associated with trophic ecology, habitat use, reproductive biology, and behaviour (e.g. Cichocki 1976; Winemiller *et al.* 1995; Galis & Metz 1998; Stiassny & Meyer 1999; Kornfield & Smith 2000; Rüber & Adams 2001). Ecologically significant variation in cichlids can be derived from relatively minor morphological modifications (see Stiassny 1991 for a review), leaving a seemingly limited set of morphological characters to use in phylogenetics. Despite these drawbacks, morphological analysis frequently has provided a robust picture of the higher-level evolutionary relationships of cichlids (e.g. Stiassny 1991; Lippitsch 1995; Kullander 1998). Recent molecular studies (e.g. Meyer 1993; Zardoya *et al.* 1996; Martin & Bermingham 1998; Farias *et al.* 1999; Verheyen *et al.* 2003; Sparks & Smith 2004; López-Fernández *et al.* 2005), including some that combine molecular and morphological data (Farias *et al.* 2000, 2001) have largely agreed with cichlid relationships derived from morphological data.

Independently derived molecular data offer a broader context for the exploration of underlying homology in seemingly homoplasious morphological data. From the interaction of molecular and morphological datasets, congruence of homologous characters should emerge, allowing morphology to contribute to overall phylogenetic resolution (e.g. Chippindale & Wiens 1994; Wiens & Reeder 1995; Baker & DeSalle 1997; Baker *et al.* 1998; Hillis & Wiens 2000). Although incongruence may occur among separate analyses of different data (e.g. Brower *et al.* 1996), it cannot be predicted *a priori*. Only a combined analysis can uncover underlying homology from character partitions that appear homoplastic when examined separately (Cognato & Vogler 2001; Damgaard & Cognato 2003; Hodges & Zamudio 2004). A so-called 'total evidence' approach, combining available molecular and morphological data, should favour the emergence of congruent phylogenetic signal above the pervasive homoplasy of cichlid morphology, resulting in the robust phylogenetic framework needed to understand cichlid evolution. Building upon improved understanding of higher-level relationships, the next logical step is to clarify the phylogeny within groups of cichlids. Large numbers of morphological characters, derived from taxonomic and high-level phylogeny studies, are potentially available for the analysis of clades within the Cichlidae (e.g. Pellegrin 1904; Regan 1905a,b; Cichocki 1976; Greenwood 1979; Stiassny 1981, 1987, 1991; Kullander 1983, 1998; Oliver 1984; Casciotta & Arratia 1993a,b; Schliewen & Stiassny 2003). The combination of diverse morphological information, along with available molecular datasets should provide resolved and well-supported hypotheses of relationships within groups of cichlids.

The subfamily Geophaginae was formally proposed by Kullander (1998) based on a morphological phylogenetic analysis

of Neotropical taxa. In his classification, the subfamily included 16 genera divided into three tribes: Acarichthyini (genera *Acarichthys* and *Guianacara*), Crenicaratini (*Biotocetus*, *Crenicara*, *Dicrossus*, and *Mazarunia*), and Geophagini (*Geophagus*, *Mikrogeophagus*, '*Geophagus*' *brasiliensis*, '*Geophagus*' *steindachneri*, *Gymnogeophagus*, *Satanoperca*, *Biotodoma*, *Apistogramma*, *Apistogrammoides*, and *Taeniacara*). In Kullander's analysis, Geophaginae was sister to the subfamily Cichlasomatinae, which included most of the remaining Neotropical cichlid diversity; the genera *Retroculus* (tribe Retroculinae), *Cichla* and *Crenicichla* (Cichlinae), *Astronotus* and *Chaetobranchius* (Astronotinae), and the African *Heterochromis*, were arrayed at the base of a paraphyletic Neotropical cichlid assemblage.

Molecular (Farias *et al.* 1999; Sparks & Smith 2004; López-Fernández *et al.* 2005) and total evidence studies including Kullander's morphological data (Farias *et al.* 2000, 2001), however, have challenged the above classification. Farias *et al.* (1999, 2000, 2001), repeatedly found the Neotropical Cichlidae to be monophyletic and *Heterochromis* to be basal to the African clade. The genera *Crenicichla* and *Teleocichla* were nested within Geophaginae (Farias *et al.* 1999, 2000, 2001; López-Fernández *et al.* 2005; Sparks & Smith 2004), expanding the limits of the subfamily, and challenging a proposed relationship between *Crenicichla*, *Teleocichla* and the basal genus *Cichla* (Cichocki 1976; Stiassny 1987, 1991).

In this paper, molecular data from three mitochondrial and three nuclear loci are combined with a new and extensive morphological dataset of geophagine cichlids, aiming at resolving the generic relationships within the subfamily. The morphological dataset was combined with the molecular matrix analysed by López-Fernández *et al.* (2005) in a combined analysis of over 4000 characters. The main goal of this paper is to improve resolution and support for the genus-level phylogeny of geophagine cichlids by incorporating morphological information. Additionally, the topologies produced by molecular, morphological, and combined data are contrasted, congruence among different partitions of molecular and morphological data is analysed, and the potential role that character incongruence and patterns of geophagine evolution may have on the phylogenetic inference of relationships within the clade is discussed.

Methods

Taxon sampling

DNA sequence data and morphological characters were collected for 38 species in 21 genera of Neotropical cichlids. Ingroup taxa included 30 species and 16 of the 18 genera of the subfamily Geophaginae (Farias *et al.* 1999, 2000, 2001; López-Fernández *et al.* 2005). *Teleocichla* and *Mazarunia* were not included in the study because specimens and tissue samples were not available. *Geophagus sensu lato* was divided into *Geophagus sensu stricto*, '*Geophagus*' *brasiliensis* and '*Geophagus*'

steindachneri (Kullander 1986; López-Fernández *et al.* 2005). The latter two are undescribed genera, each including several species. One species of each of the genera *Cichlasoma*, *Mesonauta* and *Hoplarchus* were added to the ingroup to test geophagine monophyly against the closely related subfamily Cichlasomatinae (Kullander 1998; Farias *et al.* 1999, 2000, 2001). Outgroup taxa included three species of *Cichla* and one of *Astronotus* and *Retroculus*, respectively (Oliver 1984; Stiassny 1991; Kullander 1998; Farias *et al.* 1999, 2000, 2001; Sparks & Smith 2004). Throughout the paper, the terms ingroup and outgroup will refer to the above listing of taxa.

Molecular dataset

DNA data consisted of a combined matrix of three mitochondrial and three nuclear genes totalling 3960 nucleotides (López-Fernández *et al.* 2005). The molecular dataset included sequences of the nuclear gene RAG2 for all species, and of the mitochondrial gene ND4 for 36 of 38 taxa. Additionally, it contained published sequences of the mitochondrial genes 16S and cytochrome *b* (cyt *b*), the microsatellite flanking region *Tmo-M27*, and the nuclear marker *Tmo-4C4* for most geophagine genera. Due to differences in taxon sampling among published studies and this study, sequences of different species were combined in order to increase resolution at the generic level. Details of DNA sequencing protocols, alignment, matrix construction, and accession numbers are given in López-Fernández *et al.* (2005).

Morphological dataset

One hundred and thirty-six characters from both external morphology and osteology were analysed separately and in combination with the molecular dataset. Many external morphological characters were based on Lippitsch (1993). A few were added from the descriptions of lateral line configuration in Webb (1990), and previous descriptions of colour pattern (Kullander 1986, 1990, 1998; Kullander & Ferreira 1988; Kullander & Nijssen 1989; Kullander & Silfvergrip 1991; Kullander *et al.* 1992). Osteological characters were based on a revision of the extensive literature on cichlid morphology, derived mostly from Cichocki (1976), Oliver (1984), Stiassny (1987, 1991), Casciotta & Arratia (1993a) and Kullander (1998). Additionally, our revision of geophagine morphological diversity produced several novel characters. Descriptions of morphological characters, illustrations, and detailed bibliographic references are given in Appendix 1.

Most morphology-based efforts to elucidate cichlid phylogenies have focused on higher-level relationships within the family (e.g. Stiassny 1987, 1991), or within large clades, such as the African (e.g. Oliver 1984; Lippitsch 1993, 1995), Neotropical (e.g. Cichocki 1976; Casciotta & Arratia 1993a), or both (Kullander 1998). Additionally, extensive descriptions of characters have been published, but not included in formal phylogenetic analyses (e.g. Pellegrin 1904; Regan 1920;

Kullander 1980, 1983, 1986, 1990; Kullander & Nijssen 1989). A significant portion of these studies was reviewed in search of previously proposed characters that could be of relevance for establishing the phylogeny of Geophaginae. Understandably, these studies present a diversity of approaches to character description, often lack uniformity in nomenclature, and sometimes have described characters in a way that does not allow their direct use in phylogenetics. Numerous characters were redescribed such that they could be used in the context of the present analysis. Characters that did not vary within the taxa examined were excluded, and in some cases, the original characters were split into several characters to facilitate coding or clarify the delimitation of character states (Appendix 1).

Description and scoring of characters derived from external morphology were based on direct observation of formalin-fixed, ethanol-preserved specimens. Meristic characters were evaluated on both sides of each specimen to account for variability. Osteological characters were analysed in cleared and stained specimens (Taylor & Van Dyke 1985) and/or dry, articulated skeletons. Whenever possible, observations were made on several individuals per species to account for intraspecific variability. A complete list of the material examined for morphological analysis is given in Appendix 2. Detailed collection localities and other museum data for catalogued material are available from the NEODAT project website (www.neodat.org). Voucher specimens used for tissue sampling are catalogued at the American Museum of Natural History, New York.

All morphological characters were polarized using the outgroup method, keeping multistate characters unordered. Details on polarity decisions for each character are given in Appendix 1. The coded matrix of morphological characters is given in Appendix 3. Although the focus of the analysis is placed at the generic level, whenever possible several species per genus were analysed, providing explicit tests of monophyly for the genera, and facilitating coding when genera were polymorphic for a character (see Wiens 2000).

Phylogenetic analyses

The molecular dataset was analysed in a previous study (López-Fernández *et al.* 2005); thus in this paper the morphological dataset was analysed both alone and in combination with the molecular matrix from that study. Maximum parsimony (MP) analyses, both equally and successively weighted, were performed in PAUP* (Swofford 2002) using 100 replicates of heuristic search with random addition sequence and Tree Bisection and Reconnection branch swapping (TBR). In previous analyses of the molecular data (López-Fernández *et al.* 2005), transition to transversion ratios were used to reweight characters under MP, but morphological data do not allow for an equivalent weighting rationale. Given this limitation, *a posteriori* differential weighting was performed (Chippindale & Wiens 1994: 286) by successive approximation (SA)

	Combined analysis		Partitioned Bremer support						
	BS	DI	Morphology	RAG2	Tmo-M27	Tmo-4C4	Cyt <i>b</i>	16S	ND4
Node 1	< 50	1	0	7	0	0.5	-17.5	3	8
Node 2	96	12	2.7	11.8	0	3.2	-9.7	-2.2	6.2
Node 3	< 50	0	-7	3.5	0	-0.5	-3.5	3	4.5
Node 4	< 50	0	-7	3.5	0	-0.5	-3.5	3	4.5
Node 5	< 50	0	-7	3.5	0	-0.5	-3.5	3	4.5
Node 6	< 50	3	8.5	3.5	0	2	-7.5	-0.5	-3
Node 7	< 50	0	-7	3.5	0	-0.5	-3.5	3	4.5
Node 8	72	6	10.5	-5	0	1.5	3.5	-2.5	-2
Node 9	< 50	0	-7	3.5	0	-0.5	-3.5	3	4.5
Node 10	97	20	1	16.5	3	9.5	-7.5	5	-7.5
Node 11	< 50	0	-7	3.5	0	-0.5	-3.5	3	4.5
Node 12	< 50	0	-7	3.5	0	-0.5	-3.5	3	4.5
Node 13	< 50	1	0	7	0	0.5	-17.5	3	8
Node 14	100	18	11	6.5	1	-0.5	-15.5	5	10.5
Node 15	99	22	2	11.5	0	1.5	-12.5	4	15.5
Node 16	98	17	-5	14.5	-1	2.5	-11.5	3	14.5
Node 17	77	5	2	3.5	1	-0.5	-11.5	3	7.5
Node 18	99	15	-4.5	7.5	0	0.5	-4	3	12.5
Total			-20.8	108.8	4	17.2	-135.7	44.8	101.7

Table 1 Support for genus-level tree obtained from combined analysis through successive approximation (Fig. 1B). BS = Bootstrap values, DI = Bremer support values (Decay Index). Partitioned Bremer support values for each partition are shown. Node numbers refer to node labels in Fig. 1B.

analyses (Farris 1969), using the maximum value of the rescaled consistency index (rc) of each character as implemented in PAUP*. SA favours topologies in which homoplasy of the most consistent characters is minimized (Chase & Palmer 1997), thus helping reduce the effect of sequence saturation and rate heterogeneity in the molecular data, and assigning higher weights to the least homoplastic characters in the morphological dataset (Felsenstein 2004). Support for MP-derived topologies was estimated with nonparametric bootstrap (Felsenstein 1985) and Bremer support indices (Bremer 1988, 1994) with searches performed in PAUP*. Bootstrap values were derived from 100 pseudoreplicates, each with 10 heuristic searches using random addition sequence and TBR. Bremer support was estimated using topological constraints implemented in MacClade (Maddison & Maddison 2000) under the same conditions of the original heuristic search in PAUP*.

Analyses of congruence among partitions

Congruence among the seven data partitions (i.e. Morphology, ND4, *cyt b*, 16S, RAG2, *Tmo-M27*, and *Tmo-4C4*) was estimated both *a priori* and *a posteriori* using Partition Homogeneity Tests (PHT, Farris *et al.* 1994; Swofford 1995) and Partitioned Bremer Support (PBS, Baker & DeSalle 1997; Baker *et al.* 1998), respectively. A PHT was additionally used to estimate congruence between morphological and molecular data. Because the PHT permutation test cannot be performed when data are partially missing from a partition, we eliminated all taxa with no data for one or more partitions. For tests involving Morphology, RAG2, and ND4, we excluded *Crenicara punctulatum* and *Gymnogeophagus balzanii*, for which ND4 sequences

were not available. All other tests were performed on a matrix of 14 taxa for which all molecular data were available (see López-Fernández *et al.* 2005; Table 1). We performed PHT tests among all partitions using 100 randomization cycles, each with 10 replicates of heuristic search using random addition sequence and TBR branch swapping as implemented in PAUP*.

To explore the effect of different partitions on the inferred phylogenies and to evaluate the degree of congruence between partitions *a posteriori*, the local (node level) support for each topology was compared by calculating PBS for each node (Baker & DeSalle 1997; Baker *et al.* 1998). PBS reveals if a partition in the combined analysis supports the total evidence tree, indicating how much each partition contributes to the overall Bremer support of each node. A positive value of PBS shows support for a particular node by a given partition, while a negative value indicates that the most parsimonious explanation of the data in that partition is not congruent with the combined tree. PBS values were calculated using 100 heuristic search replicates in TreeRot, v. 2 (Sorenson 1999). PBS values from the combined analysis were also used to summarize the overall congruence between each partition using the method of Sota & Vogler (2001). PBS values for each partition obtained from each simultaneous analysis were compared using Spearman's ranked correlations. A positive correlation indicates congruent support between partitions, whereas a negative correlation indicates opposing support. Lack of correlation indicates that support is not associated with the partitions being tested (Cognato & Vogler 2001; Damgaard & Cognato 2003). Spearman's correlations were calculated in SPSS version 11.0 for Windows.

Results

Partition homogeneity tests

All PHT analyses resulted in significant incongruence among partitions ($P < 0.01-0.02$). *A priori* exclusion of any data on the basis of PHT results was considered inappropriate, since PHT-based generalized incongruence does not provide justification for which partitions to exclude. PHT results were based on a dataset smaller than the one used for phylogenetic analysis, which might provide a biased evaluation of congruence due to reduced taxon sampling or lack of data. Furthermore, it has repeatedly been shown that, even in cases in which incongruence is demonstrated *a priori*, combined analyses often provide better resolved and supported trees than those derived from separate analysis of partial datasets (e.g. Cunningham 1997; Wiley *et al.* 1998). Combined parsimony

analysis should favour the emergence of underlying phylogenetic signal in the data, overriding incongruent homoplastic signal (e.g. Brower *et al.* 1996; Cognato & Vogler 2001).

Phylogenetic relationships

Morphology. One hundred and thirty-six morphological characters were analysed for all 38 taxa using both unweighted MP and SA. The unweighted analysis produced eight MP trees of 637 steps and global consistency index (CI) of 0.34, retention index (RI) of 0.64 and rescaled consistency index (RC) of 0.22. The eight alternative trees differed in the position of the genera *Geophagus*, *Satanoperca*, and *Gymnogeophagus* with respect to each other, but were otherwise identical, as was the successive approximation tree. The strict consensus tree of the morphological analysis (Fig. 1A) showed a

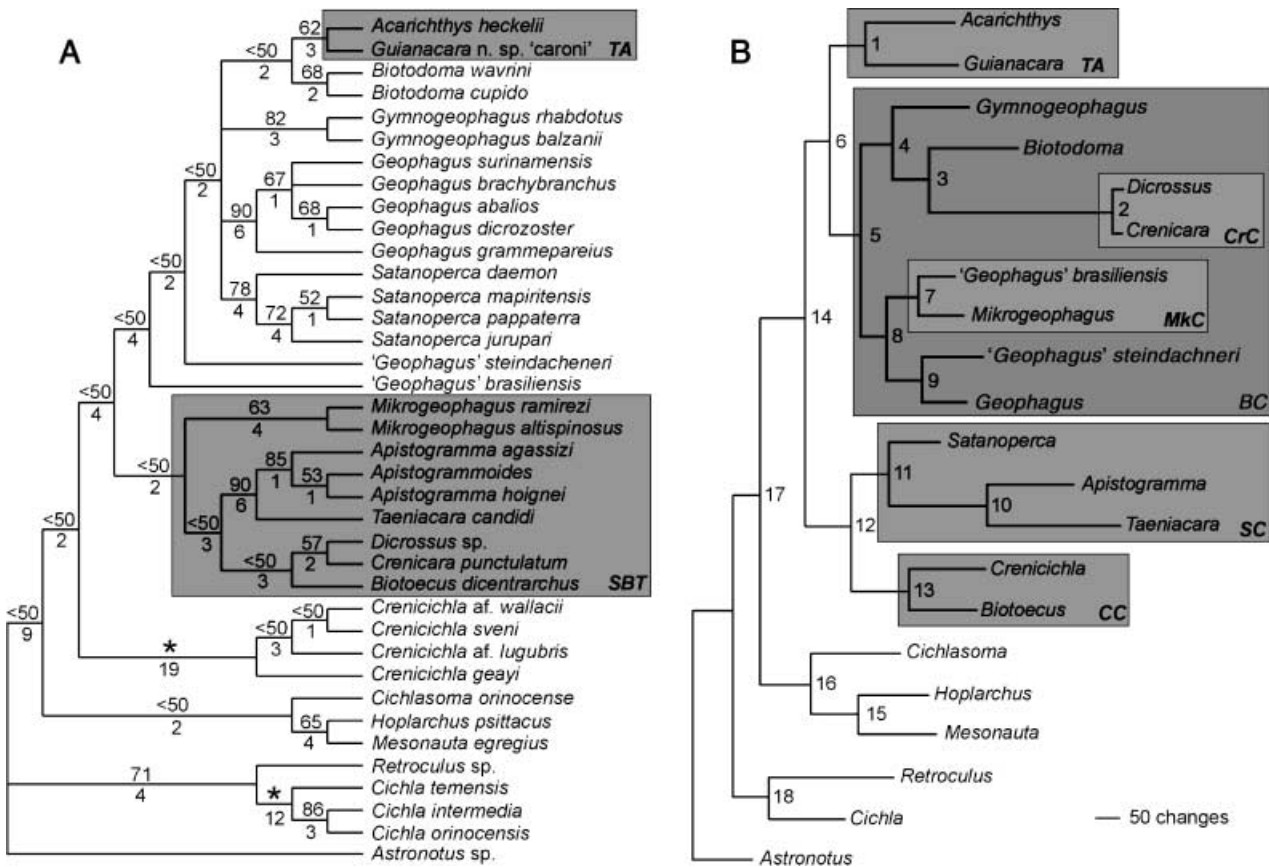


Fig. 1 A, B. Topologies from morphological and total evidence datasets. —A. Strict consensus of eight MP topologies derived from 136 equally weighted morphological characters from 38 taxa. Topologies differed in the position of the genera *Geophagus*, *Satanoperca* and *Gymnogeophagus*, but were otherwise identical, as was the successive approximation tree. Morphological data, as do molecular characters, provide strong support for the monophyly of genera. Bootstrap support based on 100 pseudoreplicates is given above branches, stars representing 100% values; Bremer support values based on 100 replicates of heuristic search are given below branches. See text for tree statistics. —B. Successive approximation topology from two MP trees derived from 4096 characters of morphology and six molecular loci (nuclear: RAG2, *Tmo-M27*, *Tmo-4C4*; mitochondrial: ND4, *cyt b*, 16S) for 38 taxa. For clarity, species-level relationships have been excluded from the figure, but all taxa were included in the analysis. Highlighted clades (see Discussion): TA = tribe Acarichthyini, SBT = Small-bodied taxa, BC = B clade, SC = *Satanoperca* clade, CC = *Crenicichla* clade, CrC = Crenicarine clade, MkC = *Mikrogeophagus* clade.

monophyletic, but weakly supported, Geophaginae including *Crenicichla*, which was placed between the nongeophagine taxa and the Geophaginae *sensu* Kullander (1998). All genera represented by more than one species were monophyletic. Most intergeneric relationships had low or moderate support, except for three clades that grouped the genera *Acarichthys* and *Guianacara* (tribe Acarichthyini [Kullander 1998] from here on), *Apistogramma* (including *Apistogrammoides*) and *Taeniacara*, and *Dicrosus* and *Crenicara* (crenicarine clade from here on), respectively.

Combined analyses. The combined analysis (CA) of the morphological and molecular datasets included 38 taxa and 4096 characters, of which 1292 were parsimony informative. The equal-weight MP analysis produced two MP trees of 6917 steps (CI = 0.33, RI = 0.42 and RC = 0.17). Both trees were completely resolved and showed a monophyletic Geophaginae, but the relationships within the subfamily were markedly different, having incongruent intergeneric relationships, and rendering the strict consensus tree unresolved at the base (not shown). The successive approximation tree was identical to one of the equal weight topologies, but support was weak for most intergeneric nodes within Geophaginae (Fig. 1B, Table 1). In general, bootstrap and global Bremer support values were congruent with each other, and strongly supported the Geophaginae (node 14), Cichlasomatinae (16), Heroini (15), a close relationship of Geophaginae and Cichlasomatinae (17), and an outgroup clade of *Cichla* and *Retroculus* (18). Within Geophaginae, the crenicarine clade and a clade uniting *Apistogramma* with *Taeniacara* were strongly supported.

Partitioned Bremer Support and modified combined analyses PBS values from the combined analyses revealed some incongruence among partitions (Table 1). Negative PBS values in at least some nodes of all partitions indicate that homoplasy is common across the data as was suggested by the PHTs. Contrary to the PHTs, however, pairwise comparisons of PBS values between partitions (Table 2) showed both positive and negative values, which indicate that even though there is incongruence among partitions, there are also important elements of agreement in their phylogenetic information.

Significantly positive correlations among several partitions indicate strong congruence within the data. Significantly negative correlations were all associated with the *cyt b* partition. *Cyt b* was significantly incongruent with RAG2, ND4, and morphology. Correlations to all other partitions also were negative, albeit nonsignificant. A PHT of *cyt b* against all other partitions was also significantly incongruent ($P < 0.01$). No other partition showed a similarly consistent negative correlation with the remainder of the data; the phylogenetic signal in *cyt b* appears to be in strong conflict with the remainder of the current dataset. To explore the effects of this incongruence, the *cyt b* partition was removed from the matrix and a simultaneous analysis was repeated in a reduced combined analysis (RCA).

The RCA dataset included all 38 taxa and 2971 characters, of which 885 were MP informative. The MP analysis resulted in two MP trees of 4876 steps (CI = 0.38, RI = 0.46 and RC = 0.18). The MP trees differed only in the position of ‘*Geophagus*’ *steindachneri*, which was alternatively placed as sister to *Gymnogeophagus* or *Geophagus sensu stricto*. The latter arrangement was supported by bootstrap analysis, but had no Bremer support (Fig. 2). The main difference between the RCA and CA trees was the grouping of *Gymnogeophagus* with *Geophagus sensu stricto* and ‘*Geophagus*’ *steindachneri* (*Geophagus* clade, GC in Fig. 2) in the former, whereas it weakly grouped with *Biotodoma* and the crenicarine clade in the CA topology (Fig. 1B). Geophagine monophyly, inclusive of *Crenicichla*, was strongly supported by the RCA analysis, and all genera were grouped into two large clades, albeit with low support. The first clade included the sister-group relationship between the tribe Acarichthyini and the B clade, formed by *Geophagus sensu lato*, *Gymnogeophagus*, *Biotodoma*, *Mikrogeophagus*, and the crenicarine clade (Fig. 2). The second clade grouped the *Satanoperca* clade with a weakly supported grouping of *Crenicichla* and *Biotoeus* (*Crenicichla* clade from here on).

Discussion

Phylogenetic relationships of Geophaginae: morphological analyses

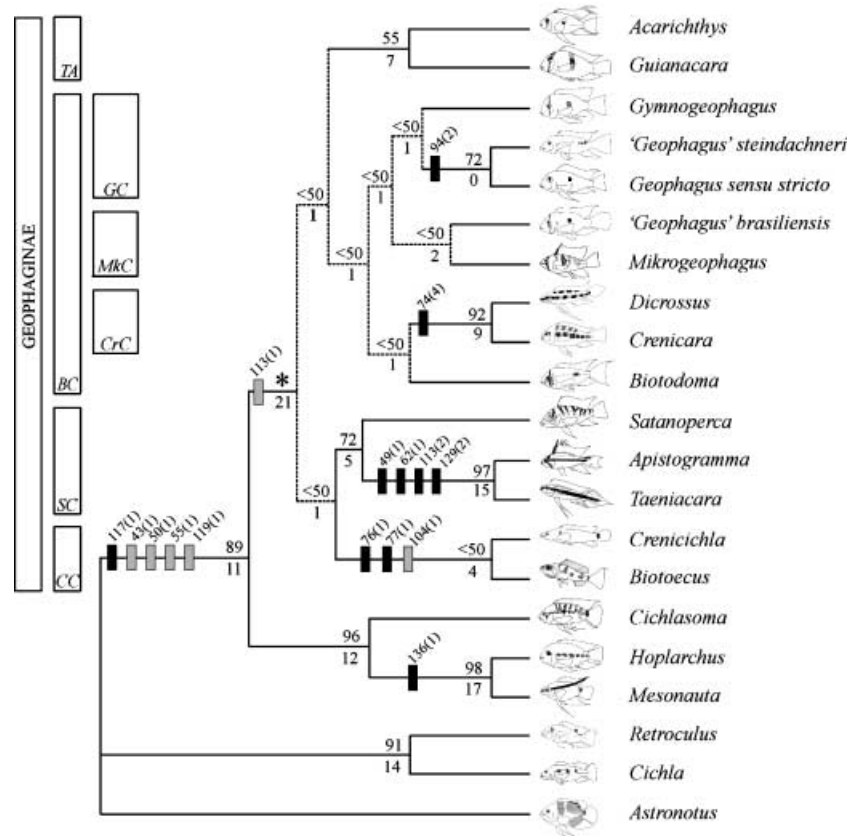
Both morphology and combined analyses resulted in a monophyletic Geophaginae, but relationships depicted were markedly

	Morphology	RAG2	Tmo-M27	Tmo-4C4	Cyt b	16S	ND4
Morphology	–	0.270	0.395	0.579*	–0.518*	–0.084	0.154
RAG2		–	0.026	0.647**	–0.696**	0.426	0.537*
Tmo-M27			–	–0.122	–0.186	0.473*	–0.213
Tmo-4C4				–	–0.375	–0.179	0.043
Cyt b					–	–0.362	–0.670**
16S						–	0.314
ND4							–

** $P < 0.01$; * $P < 0.05$.

Table 2 Pairwise Spearman’s correlation of Partitioned Bremer Support values for each partition in the successive approximation combined analysis.

Fig. 2 Topology derived from a reduced combined analysis (RCA) from which the *cyt b* partition was removed. Strict consensus topology of 2 MP trees derived from 2971 characters of morphology and five molecular loci (nuclear: *RAG2*, *Tmo-M27*, *Tmo-4C4*; mitochondrial: *ND4*, *16S*) from 38 taxa (see Methods). Species-level relationships have been excluded from the figure for clarity, but all taxa were included in the analysis. Bootstrap support based on 100 pseudoreplicates is given above branches; Bremer support values based on 100 replicates of heuristic search are given below branches. See text for tree statistics. Dotted lines highlight basal relationships with low statistical support and no morphological synapomorphies (see text for discussion). Bars represent morphological synapomorphies indicating character and derived character state numbers. Black bars indicate that a single derived state is shared by all taxa within a clade. Grey bars indicate synapomorphies whose derived state changes lower in the tree to a different derived condition. Rectangles to the left indicate clades of interest (see Discussion): *TA* = tribe Acarichthyini, *BC* = B clade, *SC* = *Satanoperca* clade, *CC* = *Crenicichla* clade, *GC* = *Geophagus* clade, *CrC* = Crenicarine clade, *MkC* = *Mikrogeophagus* clade.



different. Monophyly of all genera was supported by the morphological data (except in that *Apistogrammoides* was grouped with *Apistogramma*), thus corroborating previous molecular results (López-Fernández *et al.* 2005). When analysed alone, the morphological dataset grouped the small-bodied taxa (SBT from here on, Fig. 1A), the so-called 'dwarf cichlids', into a monophyletic clade, and failed to recover most of the intergeneric groupings found in the combined analysis. The SBT clade, including *Mikrogeophagus*, *Apistogramma*, *Taeniacara*, *Dicrossus*, *Crenicara* and *Biotoecus*, was poorly supported by six nonunique morphological synapomorphies (characters 24: 2, 51: 1, 52: 1, 53: 1, 54: 1, 110: 1). However, neither the molecular nor the combined analyses supported a SBT clade. Morphological characters supporting this clade are therefore probably correlated with body-size reduction, and do not represent secondary homologies (*sensu* de Pinna 1991). Interestingly, other studies have found that body-size reduction usually results in a parallel 'miniaturization' of certain structures, creating nonhomologous, convergent derived states (e.g. Buckup 1993). Despite *a priori* results indicating significant incongruence, the interaction of morphological characters with the molecular dataset produced different topologies than those obtained from morphology

alone and heightened support for most clades. Numerous other studies have found that the combination of morphology and molecules often produces arrangements not recovered by either data type alone, and often also increases overall support (see Brower *et al.* 1996; Baker & DeSalle 1997; Baker *et al.* 1998; Wiley *et al.* 1998; Hodges & Zamudio 2004).

A notable result of the morphological component of this study is the grouping of *Crenicichla* within Geophaginae. All previous morphological analyses (Stiassny 1987, 1991; Casciotta & Arratia 1993a; Kullander 1998) had found *Crenicichla* to be sister to *Cichla*. Stiassny (1987) analysis found both myological and osteological traits uniting the two genera, but our study revealed several of Stiassny (1987) osteological characters to be variable, both in and outside *Cichla* and *Crenicichla* (e.g. urohyal morphology, Stiassny's character 2, was not included in this study because its high variability did not allow for a satisfactory coding scheme). In some cases, new character states were identified, with the consequence of reducing support for the former hypothesis (e.g. vomerine head morphology, Stiassny's character 5; character 88 in Appendix 1). Herein, morphological support for an alignment of *Crenicichla* and the Geophaginae is found in the shared possession of a reduced number of concavities in the frayed

zone of the fourth upper pharyngeal toothplate (character 113: 1). Based on these results we predict that *Teleocichla*, sister to *Crenicichla* (Stiassny 1987; Farias et al. 2000), a taxon we have been unable to examine, also belongs in the Geophaginae.

Phylogenetic relationships of Geophaginae: combined analyses

The following paragraphs elaborate on the phylogenetic relationships of Geophaginae based on the RCA dataset (i.e. without cyt *b*). Clade nomenclature is modified after López-Fernández et al. (2005) and expanded as necessary.

The B clade. Although with low support, the RCA analysis recovered a monophyletic B clade, and within it, the *Geophagus* clade (Fig. 2), in which *Gymnogeophagus* is sister to a clade formed by ‘*Geophagus*’ *steindachneri* and *Geophagus sensu stricto*. The consistency of our molecular (López-Fernández et al. 2005; Figs 4B, 5) and RCA results (Fig. 2) suggests that the *Geophagus* clade is monophyletic, even though support for its monophyly is not overwhelming. The crenicarine clade was recovered by all analyses (Figs 1A,B, 2), even though the relationships of this group and of the genus *Biotodoma* to other geophagine genera are not well resolved. Albeit with weaker support, a monophyletic *Mikrogeophagus* clade (*Mikrogeophagus* + ‘*Geophagus*’ *brasiliensis*) was consistently recovered in all our combined analyses (Figs 1B, 2, López-Fernández et al. 2005; Figs 3–5). Unfortunately, basal relationships among the three main groups in the B clade are only tentatively established (Fig. 2, dashed lines).

The tribe Acarichthyini. Combined analysis recovered the tribe Acarichthyini (*Acarichthys* + *Guianacara*), but unlike our previous molecular analyses (López-Fernández et al. 2005), the Acarichthyini was not related to *Crenicichla* and *Biotodoma*. *Acarichthys* and *Guianacara* were grouped only by nonunique morphological synapomorphies of squamation (char. 31, reversal to state 0), colour pattern (char. 75: 1), and osteology (114: 2, 122: 1). Kullander (1998) formally proposed the tribe Acarichthyini based on characters of the first epibranchial bone (his char. 14), the lower pharyngeal jaw (his character 20), the shared expansion of the basisphenoid and the parasphenoid wing (his char. 36, and see also Kullander & Nijssen 1989), and the infraorbital series (his char. 44). Evaluation of these characters revealed wide variation and perhaps ontogenetic variability as well. Particularly, the basisphenoid expansion varies among species of *Guianacara* (e.g. *Guianacara sphenozona*, G. sp. n. ‘caroni’), and as interpreted here, the parasphenoid wing is expanded in several other taxa (e.g. *Geophagus*, and see Appendix 3). Additionally, basisphenoid shape varies independently from that of the parasphenoid. Nonetheless, the Acarichthyini is frequently recovered in both morphological and molecular analyses (Kullander 1998;

Farias et al. 1999, 2000; López-Fernández et al. 2005). Our RCA analysis also recovered the tribe (Fig. 2A,B), but without clear resolution of its relation to other geophagines.

The Crenicichla clade. *Crenicichla* and *Biotodoma* were grouped as a weakly supported clade by the CA (Fig. 1B, Table 1) and RCA analyses (Fig. 2). Despite weak statistical support, the *Crenicichla* clade is unambiguously diagnosed by the absence of divergent ridges anterior to NLF0 (76: 1), the lack of a frontal crest (77: 1), and the possession of a cartilaginous pharyngobranchial 1 (104: 1), thus showing the strongest morphological support for any clade in the tree. Interestingly, the grouping of *Crenicichla* and *Biotodoma* also was recovered by the MP analysis of the molecular data alone (López-Fernández et al. 2005: fig. 6). The relationship of the *Crenicichla* clade to other geophagines is not well resolved, but some evidence supports its sister relationship with the *Satanoperca* clade, instead of Acarichthyini, as previously suggested by molecular data (López-Fernández et al. 2005; see below).

The Satanoperca clade. A grouping of *Satanoperca*, *Apistogramma* and *Taeniacara*, is the most consistently recovered intergeneric arrangement among geophagines, but relationships to other geophagines are poorly resolved. The RCA analysis grouped the *Satanoperca* and *Crenicichla* clades, and four non-unique morphological apomorphies support that arrangement (21: 1, 61: 1, 95: 1, 131: 2). Despite these results, more evidence will be needed to corroborate whether the *Satanoperca* and *Crenicichla* clades are sister to each other. Given the contrasting ecological characteristics of the invertivorous *Satanoperca* and *Apistogramma* and the often piscivorous *Crenicichla*, the placement of the latter becomes one of the most interesting unresolved questions in the geophagine phylogeny (see below).

In summary, the RCA dataset produced the most resolved hypothesis of geophagine relationships to date (Fig. 2). Despite this, we recognize that considerable room remains for refinement of this hypothesis, and future work will focus on further resolving basal relationships that remain weakly supported and only tentatively established (Fig. 2, dashed branches). Monophyly of the Geophaginae was strongly supported by all analyses, and its close relationship with the subfamily Cichlasomatinae also was well supported (Fig. 2), including five unique morphological apomorphies (43: 1, 50: 1, 55: 1, 117: 1, 119: 1). Current evidence suggests that, within Geophaginae, two large, sister clades encompass all genera. The Acarichthyini (*Acarichthys* + *Guianacara*) is placed as sister to the B clade. Within the latter, the *Geophagus* clade (‘*Geophagus*’ *steindachneri* + *Geophagus sensu stricto*, and both sister to *Gymnogeophagus*) is sister to the *Mikrogeophagus* clade (*Mikrogeophagus* + ‘*Geophagus*’ *brasiliensis*), and in turn, the *Geophagus* and *Mikrogeophagus* clades are sister to the crenicarine clade and *Biotodoma*. The second major clade within

Geophaginae is formed by the sister relationship between the *Satanoperca* clade (*Satanoperca* + *Apistogramma* and *Taeniacara*) and the *Crenicichla* clade (*Crenicichla* + *Biotocetus*).

Phylogenetic relationships recovered in this study are derived from the largest data set and taxon sampling of geophagine cichlids available to date. Even though some of the hypothesized relationships will likely change with future study, the current topology has important implications for the definition and classification of the subfamily Geophaginae. The inclusion of the species-rich, piscivorous genus *Crenicichla* is justified herein by both molecular and morphological data and reconciles formerly opposed hypotheses of relationships (e.g. Stiassny 1987, 1991; Kullander 1998; Farias *et al.* 2000). These results confirm those of Farias *et al.* (e.g. 1999, 2000) and justify the expansion of the subfamily from 16 to 18 genera by the addition of *Crenicichla* and its sister taxon *Teleocichla*. Incorporation of *Crenicichla* and *Teleocichla* in Geophaginae makes the subfamily the largest monophyletic clade of cichlids (over 180 described species; Kullander 2003) outside those of the African great lakes. Additionally, geophagines display an array of ecomorphological specializations for feeding and habitat use and a variety of life history strategies comparable to those of the African radiations (Winemiller *et al.* 1995; López-Fernández *et al.* 2005). The addition of *Crenicichla*, with numerous piscivorous species, and of *Teleocichla*, one of few reophilic Neotropical cichlids, broadens the remarkable ecological versatility encompassed by geophagines, and highlights the potential importance of riverine taxa in understanding the evolutionary processes generating the notable diversity of cichlid fishes.

Our results strongly challenge the reality of the subfamily Cichlinae (*Cichla*, *Crenicichla*, *Teleocichla*) formalized by Kullander (1998), thus leaving the relationships of the enigmatic *Cichla* in need of further study. The suggestion that *Cichla* may be related to *Retroculus* (e.g. Fig. 2, but see Farias *et al.* 2000) requires a detailed study of basal relationships among cichlids with extensive taxon sampling from all continents (Landim, in prep.). The tribe Acarichthyini (Kullander 1998) is well supported, and appears to be related to the B clade, but a more extensive analysis of morphological variation within *Guianacara* is needed to better understand the morphological support for the group, as only a single species of *Acarichthys* is currently known. The relationship of *Crenicichla* with *Biotocetus* and the monophyly of the B clade suggest that the tribes Crenicaratini and Geophagini, as proposed by Kullander (1998), do not reflect relationships within Geophaginae (see also López-Fernández *et al.* 2005). The Crenicaratini originally included *Dicrossus*, *Crenicara* and *Biotocetus*, but our combined analyses consistently grouped *Dicrossus* and *Crenicara* within the B clade. Kullander's Geophagini grouped all geophagine genera, with the exception of those in the Acarichthyini and Crenicaratini, but the inclusion of the crenicarine clade and

the separation of *Satanoperca* and *Apistogramma* from the B clade render Kullander's Geophagini paraphyletic.

Finally, the arrangement of lineages at the base of the geophagine tree is not entirely clear, and further data are needed to further investigate relationships at that level. Here we provisionally accept the RCA topology as our best estimate of relationships among geophagine lineages given the data currently available. This topology, despite weak statistical support for basal nodes within Geophaginae, is resolved and supported by several unambiguous morphological synapomorphies. The RCA analysis recovered relationships congruent with those from other analyses performed in this and previous studies. In light of these results, Kullander's (1998) classification of the Geophaginae is in need of revision, yet we feel it is premature to present a formal classification of the subfamily, as such revision should await a more fully resolved and strongly supported phylogenetic scheme.

The relatively weak resolution at the base of the geophagine tree, regardless of analytical treatment, suggests that low support is likely not due to a lack of data, limited taxonomic sampling, or problems associated with analytical methods, but to characteristics of geophagine evolution. Several features of geophagines may complicate the recovery of a well-supported phylogeny, yet offer important insight into the evolutionary history of this species-rich and ecologically diverse group of Neotropical cichlids.

Limitations for the resolution of geophagine phylogeny

Incongruence. Despite *a priori* indications of highly incongruent partitions (i.e. PHT results), most partitions demonstrated a largely compatible phylogenetic signal. Removal of the *cyt b* partition based on PBS results resulted in a slight change of topology and a moderate but overall increase in support, especially for nodes within Geophaginae (Figs 1B, 2, Table 1). However, it is also the case that the *cyt b*, 16S, *Tmo-M27* and *Tmo-4C4* partitions are incomplete (López-Fernández *et al.* 2005). Although MP-based analyses have frequently shown great resistance to error due to missing data (Wiens & Reeder 1995), it is not possible to predict the effect of an incomplete matrix on any particular analysis. Under combined evidence, missing data may increase incongruence of a given partition if reduced taxon sampling causes a biased representation of homoplasy and/or homology within the data. PBS values (Table 1) suggest that the topology is dominated by the congruent signal of most partitions, treating *cyt b* characters as noninformative homoplasy. Removal of *cyt b* has a positive effect on the overall topology by increasing support for most nodes, even if the topology itself is not very different. Whether differences in support are due to the *cyt b* partition having a different evolutionary history, to the effect of missing data, or to some other source of conflict cannot be determined with the available data. In the meantime, we

prefer to provisionally accept the phylogeny obtained after removal of the *cyt b* partition, at least until a more complete dataset can be analysed and the sources of incongruence studied.

Adaptive radiation. Based on internal branch tests and analysis of patterns of DNA sequence evolution, López-Fernández *et al.* (2005) proposed that Geophaginae represent the result of an adaptive radiation of over 180 described species encompassing remarkable morphological, ecological, and reproductive diversity. At the molecular level, evolutionary rate heterogeneity, saturation of some mitochondrial nucleotide positions, and short branches at deep nodes make recovery of a well-supported phylogeny problematical. Adaptive radiations are by definition characterized by short basal branches reflecting a period of rapid differentiation associated with adaptive diversification (e.g. Hodges 1997; Jackman *et al.* 1997, 1999; Kontula *et al.* 2003; Poe & Chubb 2004).

An alternative interpretation is that short basal branches result from lack of information at the relevant level in the phylogeny. Even after removal of the *cyt b* partition, our analysis of geophagine relationships includes multiple species representation of the great majority of genera within the subfamily, nearly 3000 base pairs from five different loci, and a substantial morphological dataset. We believe it is unlikely that low support for basal branches results from lack of data. Addition of morphological information provided additional support for several nodes, but with the exception of the *Crenicichla* clade, the incorporation of a large number of morphological characters did not significantly improve support for relationships at the base of the tree with respect to the molecular topology. This finding supports the notion that, as at the molecular level, morphological differentiation of geophagine lineages perhaps occurred rapidly at the beginning of the radiation, leaving few characters to resolve the basal relationships within the group.

Geophaginae appear to have experienced extensive parallelisms at the morphological level (e.g. multiple independent miniaturization, see above), adding to the pervasive homoplasy within the clade. The combination of short branches, heterogeneous rates of molecular evolution, and morphological homoplasy undoubtedly hinders the process of phylogenetic inference, and complicates the estimation of a well-supported phylogeny (e.g. Felsenstein 1978; Tateno *et al.* 1982; Hillis & Wiens 2000). Nonetheless, the possibility remains that the intrinsic characteristics of the geophagine radiation render strong resolution and support for the phylogeny unattainable. A phylogeny difficult to recover is part of a complex evolutionary puzzle in which morphological, ecological, and behavioural diversity are also fundamental. Integrating phylogenetics with a clear understanding of the biology of these fishes should reveal the evolutionary processes behind

this virtually unexplored adaptive radiation, the results of which now dominate the cichlid fauna of the Neotropics.

Acknowledgements

For the loan of museum specimens and/or tissue samples we are indebted to D.C. Taphorn (Museo de Ciencias Naturales de Guanare, Venezuela), E. Pellegrini Caramaschi and P. Buckup (Universidade Federal and Museu Nacional de Rio de Janeiro), F. Pezold (North-east Louisiana University, Monroe), J. McEachran and H. Prestridge (Texas Cooperative Wildlife Collection, College Station), P. Campbell (British Museum (Natural History), England), Y. Fermon (Muséum National d'Histoire Naturelle, France), S. Willis and N. Lovejoy (University of Manitoba, Canada), I. Farias (Universidade Federal do Amazonas, Brazil), E. Revaldaves (Universidade Estadual de Maringá, Brazil). Field work in Venezuela was possible thanks to constant support from D. Taphorn (MCNG) and C. Marzuola and E. Peláez from the Cinaruco Fishing Club. Field collections in Venezuela were partially funded by grants from the National Geographic Society to KOW. Fishing permits to HLF and KOW were provided by the Servicio Autónomo de Recursos Pesqueros y Acuícolas from the Venezuelan Ministerio de Agricultura y Cría. We thank S. Willis, D. A. Arrington, C. Layman, C. Montaña, T. Turner, H. Julio, F. Pezold, J. Cotner, J. V. Montoya, C. Marzuola, J. Walther, L. Kelso-Winemiller, H. and D. López, and J. Arrington for their able field help.

Museum research was partially funded by a Collection Study Grant from the American Museum of Natural History, New York, and two Axelrod Fellowships from the Department of Ichthyology at the AMNH to HLF. HLF gratefully thanks the staff at the AMNH, MCNG and TCWC for their help during visits to the museums. Molecular laboratory work was partially funded by a Jordan Endowment Fellowship from the American Cichlid Association to HLF, and by grants from the National Science Foundation to RLH and KOW. A. Cognato suggested the use of Partitioned Bremer Support, and A. Harlin-Cognato, C. Ingram, L. Smith, T. Hrbek, I. Farias, and L. Frabotta provided ideas and frequent opportunity for discussions that helped shape this paper. Comments from two anonymous reviewers significantly improved the original version of the manuscript.

References

- Baker, R. & DeSalle, R. (1997). Multiple sources of character information and the phylogeny of Hawaiian drosophilids. *Systematic Biology*, **46**, 654–673.
- Baker, R., Yu, X. & DeSalle, R. (1998). Assessing the relative contribution of molecular and morphological characters in simultaneous analysis trees. *Molecular Phylogenetics and Evolution*, **9**, 427–436.
- Barel, C. D. N., Van Oijen, M. J. P., Witte, F. & Witte-Maas, E. (1977). An introduction to the taxonomy and morphology of the

- haplochromine Cichlidae from Lake Victoria. *Netherlands Journal of Zoology*, 27, 1–65.
- Bremer, K. (1988). The limits of amino-acid sequence data in angiosperm phylogenetic reconstruction. *Evolution*, 42, 795–803.
- Bremer, K. (1994). Branch support and tree stability. *Cladistics*, 10, 295–304.
- Brower, A. V. Z., DeSalle, R. & Vogler, A. P. (1996). Gene trees, species trees and systematics: a cladistic perspective. *Annual Review of Ecology and Systematics*, 27, 423–450.
- Buckup, P. (1993). Phylogenetic interrelationships and reductive evolution in neotropical characidiin fishes (Characiformes, Ostoriphyssi). *Cladistics*, 9, 305–341.
- Casciotta, J. & Arratia, G. (1993a). Tertiary cichlid fishes from Argentina and reassessment of the phylogeny of New World cichlids (Perciformes: Labroidei). *Kaupia*, 2, 195–240.
- Casciotta, J. R. & Arratia, G. (1993b). Jaws and teeth of American cichlids. *Journal of Morphology*, 217, 1–36.
- Chase, M. W. & Palmer, J. D. (1997). Leapfrog radiation in floral and vegetative traits among twig epiphytes in the orchid subtribe Oncidiinae. In T. J. Givnish & K. J. Sytsma (Eds) *Molecular Evolution and Adaptive Radiation* (pp. 331–352). Cambridge: Cambridge University Press.
- Chippindale, P. & Wiens, J. A. (1994). Weighting, partitioning, and combining characters in phylogenetic analysis. *Systematic Biology*, 43, 278–287.
- Cichocki, F. (1976). *Cladistic history of cichlid fishes and reproductive strategies of the American genera *Acarichthys*, *Biotodoma* and *Geophagus**. PhD Diss. Ann Arbor: The University of Michigan.
- Cognato, A. & Vogler, A. P. (2001). Exploring data interaction and nucleotide alignment in a multiple gene analysis of *Ips* (Coleoptera: Scolytinae). *Systematic Biology*, 50, 758–780.
- Cunningham, C. (1997). Can tree incongruence tests predict when data should be combined? *Molecular Biology and Evolution*, 14, 733–740.
- Damgaard, J. & Cognato, A. (2003). Sources of character conflict in a clade of water striders (Heteroptera: Gerridae). *Cladistics*, 19, 512–526.
- Farris, J. S. (1969). A successive approximation approach to character weighting. *Systematic Zoology*, 18, 374–385.
- Farias, I. P., Ortí, G. & Meyer, A. (2000). Total evidence: molecules, morphology, and the phylogenetics of cichlid fishes. *Journal of Experimental Zoology*, 288, 76–92.
- Farias, I. P., Ortí, G., Sampaio, I., Schneider, H. & Meyer, A. (1999). Mitochondrial DNA phylogeny of the family Cichlidae: monophyly and fast molecular evolution of the Neotropical assemblage. *Journal of Molecular Evolution*, 48, 703–711.
- Farias, I. P., Ortí, G., Sampaio, I., Schneider, H. & Meyer, A. (2001). The Cytochrome *b* gene as a phylogenetic marker: the limits of resolution for analyzing relationships among cichlid fishes. *Journal of Molecular Evolution*, 53, 89–103.
- Farris, J. S., Källersjö, A. G., Kluge, A. G. & Bult, C. (1994). Testing significance of incongruence. *Cladistics*, 10, 315–319.
- Felsenstein, J. (1978). Cases in which parsimony or compatibility methods will be positively misleading. *Systematic Zoology*, 27, 401–410.
- Felsenstein, J. (1985). Confidence limits on phylogenies: an approach using the bootstrap. *Evolution*, 39, 783–791.
- Felsenstein, J. (2004). *Inferring Phylogenies*. Sunderland, MA: Sinauer.
- Galis, F. & Metz, J. (1998). Why are there so many cichlid species? *Trends in Ecology and Evolution*, 13, 1–2.
- Greenwood, P. H. (1979). Towards a phyletic classification of the ‘genus’ *Haplochromis* (Pisces, Cichlidae) and related taxa. Part I. *Bulletin of the British Museum (Natural History) Zoology Series*, 35, 265–322.
- Hillis, D. M. & Wiens, J. J. (2000). Molecules versus morphology in systematics: conflicts, artifacts, and misconceptions. In J. J. Wiens (Ed.) *Phylogenetic Analysis of Morphological Data* (pp. 1–19). Washington DC: Smithsonian Institution Press.
- Hodges, S. (1997). Rapid radiation due to a key innovation in columbines (Ranunculaceae: Aquilegia). In T. J. Givnish & K. J. Sytsma (Eds) *Molecular Evolution and Adaptive Radiation* (pp. 391–406). Cambridge: Cambridge University Press.
- Hodges, W. & Zamudio, K. (2004). Horned lizard (*Phrynosoma*) phylogeny inferred from mitochondrial genes and morphological characters: understanding conflicts using multiple approaches. *Molecular Phylogenetics and Evolution*, 31, 961–971.
- Jackman, T., Larson, A., de Queiroz, K. & Losos, J. B. (1999). Phylogenetic relationships and tempo of early diversification in *Anolis* lizards. *Systematic Biology*, 48, 254–285.
- Jackman, T., Losos, J. B., Larson, A. & de Queiroz, K. (1997). Phylogenetic studies of convergent adaptive radiations in Caribbean *Anolis* lizards. In T. J. Givnish & K. J. Sytsma (Eds) *Molecular Evolution and Adaptive Radiation* (pp. 535–558). Cambridge: Cambridge University Press.
- Kontula, T., Kirilchik, S. & Väinölä, R. (2003). Endemic diversification of the monophyletic cottoid fish species flock in Lake Baikal explored with mtDNA sequencing. *Molecular Phylogenetics and Evolution*, 27, 143–155.
- Kornfield, I. & Smith, P. (2000). African cichlid fishes: Model systems for evolutionary biology. *Annual Review of Ecology and Systematics*, 31, 163–196.
- Kullander, S. O. (1980). A taxonomical study of the genus *Apistogramma* Regan, with a revision of Brazilian and Peruvian species (Teleostei: Percoidei: Cichlidae). *Bonner Zoologische Monographien*, 14, 1–152.
- Kullander, S. O. (1983). *A Revision of the South American Cichlid Genus *Cichlasoma* (Teleostei: Cichlidae)*. Stockholm: Swedish Museum of Natural History.
- Kullander, S. O. (1986). *Cichlid Fishes of the Amazon River Drainage of Peru*. Stockholm: Swedish Museum of Natural History.
- Kullander, S. O. (1990). *Mazarunia mazarunii* (Teleostei: Cichlidae), a new genus and species from Guyana, South America. *Ichthyological Exploration of Freshwaters*, 1, 3–14.
- Kullander, S. O. (1996). *Heroína isonycterina*, a new genus and species of cichlid fish from Western Amazonia, with comments on cichlasomine systematics. *Ichthyological Exploration of Freshwaters*, 7, 149–172.
- Kullander, S. O. (1998). A phylogeny and classification of the Neotropical Cichlidae (Teleostei: Perciformes). In L. R. Malabarba, R. E. Reis, R. P. Vari, Z. M. Lucena & C. A. S. Lucena (Eds) *Phylogeny and Classification of Neotropical Fishes* (pp. 461–498). Porto Alegre: EDIPUCRS.
- Kullander, S. O. (2003). Family Cichlidae (Cichlids). In R. E. Reis, S. O. Kullander & C. J. Ferraris Jr (Eds). *Check List of the Freshwater Fishes of South and Central America* (pp. 605–656). Porto Alegre: Museu de Ciências e Tecnologia — Pontifícia Universidade Católica do Rio Grande do Sul.
- Kullander, S. O. & Ferreira, E. J. G. (1988). A new *Satanoperca* species (Teleostei, Cichlidae) from the Amazon River basin in Brazil. *Cybio*, 12, 343–355.

- Kullander, S. O. & Nijssen, H. (1989). *The Cichlids of Surinam*. Leiden: E.J. Brill.
- Kullander, S. O., Royero, R. & Taphorn, D. (1992). Two new species of *Geophagus* (Teleostei: Cichlidae) from the Rio Orinoco Drainage in Venezuela. *Ichthyological Exploration of Freshwaters*, 3, 359–375.
- Kullander, S. O. & Silfvergrip, A. M. C. (1991). Review of the South American cichlid genus *Mesonauta* Gunther (Teleostei, Cichlidae) with descriptions of two new species. *Revue Suisse de Zoologie*, 98, 407–448.
- Kullander, S. O. & Staeck, W. (1990). *Crenicara latruncularium* (Teleostei, Cichlidae), a new cichlid species from Brazil and Bolivia. *Cybiurn*, 14, 161–173.
- Lippitsch, E. (1990). Scale morphology and squamation patterns in cichlids (Teleostei, Perciformes): A comparative study. *Journal of Fish Biology*, 37, 265–291.
- Lippitsch, E. (1993). A phyletic study on lacustrine haplochromine fishes (Perciformes, Cichlidae) of East Africa, based on scale and squamation characters. *Journal of Fish Biology*, 42, 903–946.
- Lippitsch, E. (1995). Scale and squamation character polarity and phyletic assessment in the family cichlidae. *Journal of Fish Biology*, 47, 91–106.
- López-Fernández, H., Honeycutt, R. L. & Winemiller, K. O. (2005). Molecular phylogeny and evidence for an adaptive radiation of geophagine cichlids from South America (Perciformes: Labroidae). *Molecular Phylogenetics and Evolution*, 34, 227–244.
- Maddison, W. & Maddison, D. R. (2000). *MacClade: Analysis of Phylogeny and Character Evolution*, Version 4.0. Sunderland, Massachusetts: Sinauer.
- Martin, A. P. & Bermingham, E. (1998). Systematics and evolution of Lower Central American Cichlids inferred from analysis of Cytchrome *b* gene sequences. *Molecular Phylogenetics and Evolution*, 9, 192–203.
- Meyer, A. (1993). Phylogenetic relationships and evolutionary processes in East African cichlid fishes. *Trends in Ecology and Evolution*, 8, 279–284.
- Oliver, M. (1984). *Systematics of African cichlid fishes: determination of the most primitive taxon, and studies on the haplochromines of Lake Malawi*. PhD Diss. Yale University.
- Pellegrin, J. (1904). Contribution à l'étude anatomique, biologique et taxonomique de poissons de la famille des Cichlidés. *Mémoire de la Société Zoologique de France*, 16, 41–399.
- de Pinna, M. G. G. (1991). Concepts and tests of homology in the cladistic paradigm. *Cladistics*, 7, 367–394.
- Poe, S. & Chubb, A. (2004). Birds in a bush: five genes indicate explosive evolution of avian orders. *Evolution*, 58, 404–415.
- Regan, C. T. (1905a). A revision of the South-American cichlid genera *Crenicara*, *Batrachops*, and *Crenicichla*. *Proceedings of the Zoological Society of London*, 1, 152–168.
- Regan, C. T. (1905b). A revision of the fishes of the South-American cichlid genera *Acara*, *Nannacara*, *Acaropsis*, and *Astronotus*. *Annals and Magazine of Natural History*, 88, 329–347.
- Regan, C. T. (1920). The classification of the fishes of the family Cichlidae. I. The Tanganyika genera. *The Annals and Magazine of Natural History*, 9, 33–53.
- Rüber, L. & Adams, D. (2001). Evolutionary convergence of body shape and trophic morphology in cichlids from Lake Tanganyika. *Journal of Evolutionary Biology*, 14, 325–332.
- Schliwien, U.K. & Stiassny, M. L. J. (2003). *Etia nguti*, a new genus and species of cichlid fish from the River Mamfue, Upper Cross River basin in Cameroon, West-Central Africa. *Ichthyological Exploration of Freshwaters*, 14, 61–71.
- Sorenson, M. (1999). *Treerot*, Version 2. Boston, Massachusetts: Boston University.
- Sota, T. & Vogler, A. P. (2001). Incongruence of mitochondrial and nuclear gene trees in the carabid beetles *Obomopterus*. *Systematic Biology*, 50, 39–59.
- Sparks, J. S. & Smith, W. (2004). Phylogeny and biogeography of cichlid fishes (Teleostei: Perciformes: Cichlidae). *Cladistics*, 20, 501–517.
- Stiassny, M. L. J. (1981). The phyletic status of the family Cichlidae (Pisces: Perciformes): a comparative anatomical investigation. *Netherlands Journal of Zoology*, 31, 275–314.
- Stiassny, M. L. J. (1987). Cichlid familial intrarelationships and the placement of the neotropical genus *Cichla* (Perciformes, Labroidae). *Journal of Natural History*, 21, 1311–1331.
- Stiassny, M. L. J. (1991). Phylogenetic intrarelationships of the family Cichlidae: an overview. In M. H. A. Keenleyside (Ed.) *Cichlid Fishes: Behaviour, Ecology and Evolution* (pp. 1–35). London: Chapman Hall.
- Stiassny, M. L. J. (1992). Atavisms, phylogenetic character reversals, and the origin of evolutionary novelties. *Netherlands Journal of Zoology*, 42, 260–276.
- Stiassny, M. L. J. & Meyer, A. (1999). Cichlids of the Rift Lakes. *Scientific American*, 280, 64–69.
- Swofford, D. L. (2002). *PAUP* Phylogenetic Analysis Using Parsimony (*and Other Methods)*, Version 4.0b10. Sunderland, Massachusetts: Sinauer.
- Tateno, Y., Nei, M. & Tajima, F. (1982). Accuracy of estimated phylogenetic trees from molecular data. I. Distantly related species. *Journal of Molecular Evolution*, 18, 387–404.
- Taylor, W. & Van Dyke, G. (1985). Revised procedures for staining and clearing small fishes and other vertebrates for bone and cartilage study. *Cybiurn*, 9, 107–119.
- Verheyen, E., Salzburger, W., Snoeks, J. & Meyer, A. (2003). Origin of the superflock of cichlid fishes from Lake Victoria, East Africa. *Science*, 300, 325–329.
- Webb, J. F. (1990). Ontogeny and phylogeny of the trunk lateral line system in cichlid fishes. *Journal of Zoology (London)*, 221, 405–418.
- Wiens, J. J. (2000). Coding morphological variation within species and higher taxa for phylogenetic analyses. In J. J. Wiens (Ed.) *Phylogenetic Analysis of Morphological Data* (pp. 115–145). Washington DC: Smithsonian Institution Press.
- Wiens, J. & Reeder, T. (1995). Combining data sets with different numbers of taxa for phylogenetic analysis. *Systematic Biology*, 44, 548–558.
- Wiley, E., Johnson, G. D. & Dimmick, W. W. (1998). The phylogenetic relationships of lampridiform fishes (Teleostei: Acanthomorpha), based on total-evidence analysis of morphological and molecular data. *Molecular Phylogenetics and Evolution*, 10, 417–425.
- Winemiller, K. O., Kelso-Winemiller, L. C. & Brenkert, A. L. (1995). Ecomorphological diversification and convergence in fluvial cichlid fishes. *Environmental Biology of Fishes*, 44, 235–261.
- Zardoya, R., Vollmer, D., Craddock, C., Streelman, J., Karl, S. & Meyer, A. (1996). Evolutionary conservation of microsatellite flanking regions and their use in the phylogeny of cichlid fishes (Pisces: Perciformes). *Proceedings of the Royal Society of London, Series B*, 263, 1589–1598.

Appendix 1

Description of morphological characters

References to the original papers where characters were proposed are given when appropriate. To the best of our knowledge, characters without bibliographic reference are proposed here for the first time in a phylogenetic context. Numbers in brackets correspond to character states used in this paper. Refer to Appendix 3 for the coded matrix of character states in the 38 included taxa.

Squamation patterns

- 1 *Opercular squamation* (Lippitsch 1993: char. 1). [0] Fully scaled, Kullander (1986: 190, fig. 65); [1] partially scaled. State 1 does not include the naked 'opercular spot' (Lippitsch 1993), which is characteristic of most African cichlids (Stiassny 1991), but not observed in the study taxa.
- 2 *Opercular scale type* (Lippitsch 1993: char. 2, modified). [0] Cycloid; [1] ctenoid. Degrees of ctenoidi were considered as alternate character states by Lippitsch (1993); we were unable to establish clear limits between degrees of ctenoidi and have coded this character as binary.
- 3 *Subopercular squamation* (Lippitsch 1993: char. 4). [0] Fully scaled, Lippitsch (1993: 912, fig. 2a); [1] caudo-ventral rim naked, Lippitsch (1993: 912, fig. 2a). State 1 restricted to taxa in which the space between the outermost row of scales and the edge of the subopercle is wide enough to accommodate another scale row.
- 4 *Subopercular scale type* (Lippitsch 1993: char. 5, modified as char. 2). [0] Cycloid; [1] ctenoid.
- 5 *Interopercular squamation* (Lippitsch 1993: char. 6). [0] Caudo-dorsally scaled; [1] caudally scaled, Lippitsch (1993: 913, fig. 3b); [2] fully scaled, Lippitsch (1993: 913, fig. 3a); [3] scaleless.
- 6 *Interopercular scale type* (Lippitsch 1993: char. 7, modified as char. 2). [0] Cycloid; [1] ctenoid.
- 7 *Cheek squamation* (Lippitsch 1993: char. 10). [0] Fully scaled, Kullander (1986: 196, fig. 68); [1] rostral half naked; [2] rostro-ventrally naked, Kullander (1986: 130, fig. 35); [3] rostrally naked; [4] ventrally naked; [5] scaleless. A rostral half naked (state 1) implies a straight, almost vertical separation of the scaled caudal region from the rostral naked area. A rostrally naked cheek (state 3) lacks scales in the rostral-most portion of the cheek, but the naked area never extends to the middle of the cheek, and the line separating the scaled from the naked portion is irregular. A fully scaled cheek was considered the plesiomorphic state based on *Astronotus* and two of three species of *Cichla*.
- 8 *Cheek scale type* (Lippitsch 1993: char. 11, modified as char. 2). [0] Cycloid; [1] ctenoid.
- 9 *Postorbital squamation* (Lippitsch 1993: char. 12). [0] Single column, Lippitsch (1993: 915, fig. 5a); [1] more than 2 columns; [2] 2 columns, Lippitsch (1993: 915, fig. 5b). Character restricted to scales immediately behind the orbit.

The outgroup is highly variable, the plesiomorphic state was defined based on Lippitsch (1995).

- 10 *Postorbital scale type*. [0] Cycloid; [1] ctenoid.
- 11 *Size of occipital scales compared to dorsal scales* (Lippitsch 1993: char. 17, modified). [0] Smaller; [1] equal size. Dorsal scales refer to scales above the upper lateral line (ULL). Lippitsch's character was multistate, but as we could not distinguish between her 'not significant, significant, and extremely small scales' it is treated here as binary.
- 12 *Dorsal scale type* (Lippitsch 1993: char. 20, modified as char. 2). [0] Cycloid; [1] ctenoid. Polarity based on *Astronotus*, basal cichlids, and most labroids (Lippitsch 1995).
- 13 *Flank scale shape* (Lippitsch 1993: char. 25). [0] Circular; [1] ovoid, long axis vertical; [2] ovoid, long axis horizontal. Evaluated on scales below the ULL behind the caudal edge of the pectoral fin.
- 14 *Lower median of caudal peduncle squamation* (Lippitsch 1993: char. 41). [0] 3 rows; [1] 2 rows; [2] 4 rows; [3] 5 rows; [4] 6 rows; [5] 7 rows; [6] 8 rows; [7] 11 rows. Number of scale rows between the lower lateral line (LLL, not included) and the row of scales posterior to the base of the anal fin (not included). Because the character was polymorphic among outgroup taxa, polarity was based on the Malagasy cichlid *Ptychochromis*. Cichlids from Madagascar are well established as the basal members of the family (Sparks & Smith 2004), and have been used before to determine plesiomorphic states (e.g. Lippitsch 1995).
- 15 *Scales on lateral chest* (Lippitsch 1993: char. 43, modified as char. 2). [0] Ctenoid; [1] cycloid. The lateral chest area is located caudal to the gill cover, ventral to the insertion of the pectoral fin, and rostral to an imaginary line between the pectoral and pelvic fin insertions.
- 16 *Size of lateral chest scales compared to flank scales* (Lippitsch 1993: char. 44, part, modified as char. 11). [0] Smaller, Greenwood (1979: 271, fig. 1); [1] equal size, Greenwood (1979: 272, fig. 2).
- 17 *Lateral chest scale implantation* (Lippitsch 1993: char. 44, part). [0] Imbricating; [1] not imbricating.
- 18 *Chest to flank scale transition* (Lippitsch 1993: char. 45). [0] Gradual; [1] abrupt, Greenwood (1979: 272, fig. 2). In a gradual transition, scales on the chest and flank are the same size, or change in size occurs across several rows of scales. An abrupt change implies two adjacent rows of differently sized scales (see also Lippitsch 1990: 280).
- 19 *Ventral chest squamation* (Lippitsch 1993: char. 46). [0] Fully scaled; [1] scaleless. Ventral chest situated between insertion of the pelvic fins and the ventral margin of the branchiostegal membrane.
- 20 *Chest scale type* (Lippitsch 1993: char. 47, modified as char. 2). [0] Cycloid; [1] ctenoid.
- 21 *Ventral chest to lateral chest scale size* (48). [0] Smaller; [1] equal. In state 0, ventral chest scales are less than half the size of the lateral chest scales.

- 22** *Ventral chest scale implantation* (Lippitsch 1993: char. 48). [0] Imbricating; [1] not imbricating.
- 23** *Ventral to lateral chest scale transition* (Lippitsch 1993: char. 49). [0] Gradual; [1] abrupt. Evaluation as for character 18.
- 24** *Inter-pelvic squamation* (Lippitsch 1993: char. 51). [0] Irregular; [1] biserial; [2] uniserial. Interpreted after Lippitsch (1993: 915) as the number of scale rows between the insertion of the pelvic fins. Irregular arrangement has a variable number of scales in an irregular pattern, usually with several scales between the pelvics. Uniserial and biserial with one or two scale rows between the pelvic fins, respectively.
- 25** *Large interpelvic scale* (Lippitsch 1993: char. 52). [0] Absent; [1] present.
- 26** *Belly scale type* (Lippitsch 1993: char. 54, modified as char. 2). [0] Ctenoid; [1] cycloid. Belly is the area between pelvic fins insertion and the anus.
- 27** *Size of belly scales compared to flank scales* (Lippitsch 1993: char. 55). [0] Smaller; [1] equal. Evaluation as for character 16.
- 28** *Belly to flank scale transition* (Lippitsch 1993: char. 56). Gradual [0]; abrupt [1]. Evaluation as for character 18.
- 29** *Scales on anal-genital region* (Lippitsch 1993: char. 58, modified as char. 2). [0] Ctenoid; [1] cycloid. See comments on character 2. Restricted to scales immediately around anus and the urogenital papilla.
- 30** *Caudal fin squamation* (Lippitsch 1993: char. 65). [0] Fully scaled; [1] partially scaled.
- 31** *Caudal fin scale type* (Lippitsch 1993: char. 66, modified as char. 2). [0] Cycloid; [1] Ctenoid.
- 32** *Caudal fin squamation* (Lippitsch 1993: char. 67, modified). [0] Rays densely covered; [1] single rows on interradial membranes; [2] staggered rows on interradial membranes.
- 33** *Pectoral fin squamation* (Lippitsch 1993: char. 73). [0] Scaleless; [1] partially scaled. Polarity based on *Astronotus*, *Cichla intermedia*, and Lippitsch (1993).
- 34** *Dorsal fin squamation* (Lippitsch 1993: char. 60, part, modified as char. 11). [0] Scaled; [1] scaleless.
- 35** *Location of dorsal fin squamation* (Lippitsch 1993: char. 60, part). [0] Soft portion only; [1] both soft and spinous portions.
- 36** *Dorsal fin scale type* (Lippitsch 1993: char. 61, modified as char. 2). [0] Ctenoid; [1] cycloid.
- 37** *Dorsal fin squamation pattern* (Lippitsch 1993: char. 62). [0] Double or multiple rows on interradial membranes; [1] single rows on interradial membranes.
- 38** *Dorsal fin base* (Lippitsch 1993: char. 63). [0] With scaly pad; [1] without pad or sheath (Kullander *et al.* 1992: 363, fig. 2); [2] with vestigial sheath; [3] with well developed sheath (Kullander *et al.* 1992: 363, fig. 2). Here a scaly pad refers to a distinct area along the dorsal fin base with scales smaller than those on the flanks. Contrary to a sheath, the pad does not cover any portion of the fin.
- 39** *Dorsal fin pad or sheath squamation* (Lippitsch 1993: char. 64, modified as char. 2). [0] Ctenoid; [1] cycloid.
- 40** *Anal fin squamation* (Lippitsch 1993: char. 68, part). [0] Scaled; [1] scaleless.
- 41** *Anal fin scale location* (Lippitsch 1993: char. 68, part). [1] Soft portion only; [1] both soft and spiny portions. Polarity based on *Astronotus*.
- 42** *Anal fin scale type* (Lippitsch 1993: char. 69, modified as char. 2). [0] Ctenoid; [1] cycloid.
- 43** *Anal fin squamation pattern* (Lippitsch 1993: char. 70). [0] Multiple rows on interradial membranes; [1] single rows on interradial membranes.
- 44** *Anal fin base* (Lippitsch 1993: char. 71). [0] With scaly pad; [1] without pad or sheath; [2] with vestigial sheath; [3] with well developed sheath.
- 45** *Anal fin pad or sheath of anal squamation* (Lippitsch 1993: char. 72, modified as char. 2). [0] Cycloid; [1] ctenoid.

Dermal bones

- 46** *Preopercular edge*. [0] Smooth; [1] serrated. Serration of dermal bones has been used as a taxonomic character (e.g. Kullander 1980, 1990; Kullander & Staeck 1990), but not in phylogenetic analysis (but see Kullander 1990).
- 47** *Supracleithral edge*. [0] Smooth; [1] serrated.
- 48** *Post-temporal edge*. [0] Smooth; [1] serrated.

Lips

- 49** *Lower lip fold symphysis*. [0] Discontinuous; [1] continuous.
- 50** *Type of lip fold* (Stiassny 1987). [0] Type I, African; [1] type II, American. See also Kullander (1983, 1986).

Lateral line and associated squamation

- 51–54** *Configuration of neurocranial laterosensory canal pores*. [0] Multiple; [1] single. The opening of NLF0 (51), NLF1 (52), NLF2 (53) and NLF3 (54) (see Barel *et al.* 1977: 91, fig. 8) at the skin surface can have single or multiple openings. Generally, all four pores share the same state, except in *Biotodoma*, *Gymnogeophagus* and *Cichlasoma*, which suggest there is independence between pores.
- 55** *Number of preopercular laterosensory canal foramina* (Stiassny 1987, 1991: char. 17). [0] 7; [1] 6; [2] 5. See also Kullander (1998: char. 47).
- 56** *Number of laterosensory pores on the dentary* (Casciotta & Arratia 1993a: char. 15). [0] 5; [1] 4. See also Kullander (1983: char. 3, 1998, chars. 45, 46).
- 57** *Trunk canal pattern of the lateral line*. Characters 57–62 refer to or are derived from the analysis of lateral line configuration and ontogeny of Webb, and follow that nomenclature (Webb 1990: 412–413, fig. 4 and table 1). [0] D4, disjunct with rostral extension of canal (Fig. 3A); [1] D1, simple disjunct (Fig. 3B); [2] D2, disjunct with rostral extension of pitted scales (Fig. 3C); [3] D3, disjunct with rostral extension

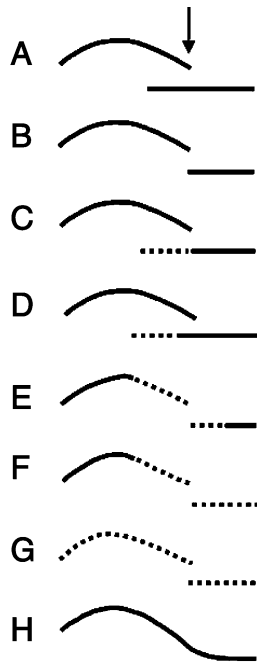


Fig. 3 A–H. Trunk canal pattern of the lateral line (char. 57, states 0–7) modified after Webb (1990: 412–413, fig. 4 and table 1). The arrow indicates the point of overlap between the upper and lower lateral line segments. See Appendix 1 for character descriptions.

of canal and pitted scales (Fig. 3D); [4] D8, Disjunct with partial replacement of canal segments by pitted scales (Fig. 3E); [5] D8.5, disjunct with complete replacement of canal segments by pitted scales on LLL (Fig. 3F); [6] D9, disjunct with complete replacement of canal segments by pitted scales on both ULL and LLL (Fig. 3G); [7] continuous lateral line (Fig. 3H). Condition D8.5 (state 5) appears restricted to *Apistogrammoides pucallpaensis*. The continuous lateral line condition (state 7) has been discussed regarding the phylogenetic position of *Cichla* (Stiassny 1981, 1987, 1991); we have considered it autapomorphic, regardless of whether it has truly arisen *de novo*, or is an atavistic expression of a basal percomorph condition (Stiassny 1992).

58 Number of overlapping tubed scales. [0] 4 or fewer; [1] 7 or more. Overlapping scales in the ULL and LLL are those located in the same column. Scales are obliquely orientated columns and are considered to be in the same column when located in the same oblique row.

59 Number of ULL pitted scales caudal to last tubed ULL scale. [0] 7 or fewer; [1] 15 or more. Scale types were evaluated following descriptions in Webb (1990: 409).

60 Scale rows between ULL and LLL. [0] 2 or 3; [1] 4 or 5. Although there is no apparent discontinuity between these two states, no taxon had an intermediate condition. Specimens of some species may have 2 or 3 (*Retroculus*), or 4 or 5 rows of

scales (*Cichla intermedia*), but we found no taxon with 3 or 4 rows.

61 Scale rows between ULL and dorsal fin origin. [0] 6–7; [1] 1; [2] 2; [3] 3; [4] 4; [5] 5; [6] 8–11; [7] 12; [8] 14; [9] 18. See comments for character 57. Count ranges include taxa with individuals with variable row numbers in range; single number states represent taxa that were invariant for scale row number.

62 Scale rows between last ULL tubed scale and base of the dorsal fin. [0] 2–5; [1] 0.5; [2] 1; [3] 11 or more. See comments for character 58. 0.5 row is counted as a single scale approximately half the size of a normal flank scale.

63 Dorsal caudal fin lateral line ramus (Kullander 1998: char. 78). [0] Absent; [1] present between caudal rays D3 and D4; [2] present between caudal rays D2 and D3.

64 Ventral caudal fin lateral line ramus. [0] Present between caudal rays V4 and V5; [1] present between caudal rays V3 and V4; [2] absent.

Color pattern

65 Caudal peduncular spot (Kullander 1998: char. 88, part). [0] Present; [1] absent. Dark mark, ocellated or not, on the base of the caudal peduncle.

66 Caudal peduncular spot position. [0] Dorsal; [1] medial.

67 Caudal spot type. [0] Ocellated; [1] simple blotch; [2] ‘*Dicrossus* band’. The *Dicrossus* band refers to a single, faint, vertical band only present in *Dicrossus* and *Biotocetus*.

68 Dorsal spot. [0] Absent; [1] present. Among Neotropical taxa, a dark blotch at the base of the soft portion of the dorsal fin is found only in *Retroculus*. Kullander indicates its presence in *Heros* (Kullander 1998) and we have observed a comparable character in some specimens of *Hoplarchus* and *Mikrogeophagus altispinosus*. It is difficult to ascertain whether the spot observed in these derived Neotropical taxa is homologous with a dorsal spot found in many African and Madagascan taxa.

69 Suborbital stripe. [0] Absent (Fig. 4A); [1] complete, extending from the lower edge of the orbit to the interopercle (Fig. 4B); [2] from the lower edge of the orbit to the preopercle (Fig. 4C); [3] limited to the cheek (Fig. 4D); [4] limited to the preopercle (Fig. 4E); [5] complete except for the preopercle (Fig. 4F).

70 Supraorbital stripe. [0] Absent; [1] directed caudad; [2] directed rostrad.

71 Postorbital stripe. [0] Absent; [1] present; [2] present, ‘*Dicrossus* type’. The ‘*Dicrossus* type’ is a triangle-shaped blotch with its base on the caudal edge of the orbit and its tip pointing caudad.

72 Preorbital stripe (Kullander 1998: char. 89, modified). [0] Absent; [1] present, ‘*Apistogramma* type’; [2] present, ‘*Dicrossus* type’. The *Apistogramma* stripe is thin, dark with smooth or irregular edges, directed rostrally, but slightly inclined ventrally; the ‘*Dicrossus* stripe’ is broad, sharp-edged and directed rostrally.

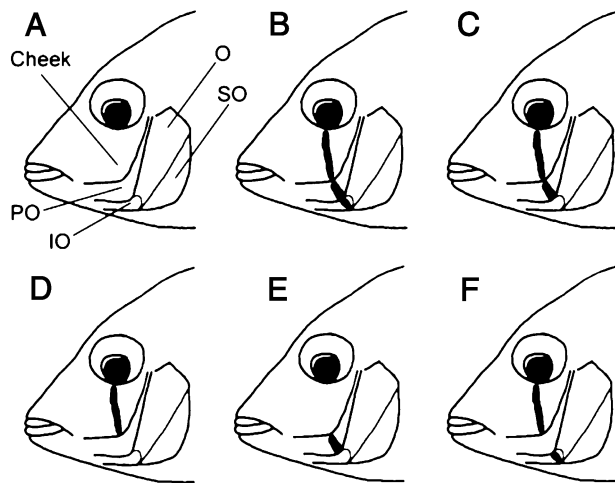


Fig. 4 A–F. Infraorbital stripe patterns (char. 69, states 0–5). *Abbreviations:* IO: interopercle; O, opercle; PO, preopercle; SO, subopercle. See Appendix 1 for character descriptions.

73 Lateral band. [0] Present; [1] absent. A lateral band is a frequently spotted dark band running from behind the opercle to the base of the caudal fin; it sometimes continues over the head as the postorbital and preorbital stripes. Character evaluation in some taxa can be confounded by ontogenetic stage; for example, in *Cichla*, the band is present in juveniles, but disappears (*C. orinocensis*, *C. temensis*) or is modified (*C. intermedia*) in adults. *Cichla* is coded based on adult specimens.

74 Body markings. [0] Faint or inconspicuous body bars; [1] spotted, interrupted midline; [2] camouflage-like; [3] barred; [4] checkerboard pattern. Most cichlids present a faint pattern of vertical bars on the flanks, and generally, the spots forming the lateral band coincide with the body bars. This character refers to melanic coloration in preserved specimens and was evaluated on several specimens. Intensity of coloration of cichlids varies strongly in live individuals.

75 First dorsal fin ray membranes. [0] Uncoloured, or indistinct from the remainder of the fin; [1] black or distinctively dark.

Neurocranium

76 Divergent frontal ridges anterior to NLF0 (Cichocki 1976: char. 3, modified). [0] Present (Fig. 5A,B); [1] absent (Fig. 5C). See also Stiassny (1991: 12–13).

77 Presence of medial frontal crest. [0] Present (Fig. 5A,B); [1] absent (Fig. 5C).

78 Composition of the pharyngeal apophysis of the basiocranium (Regan 1920). [0] Parasphenoid only; [1] parasphenoid and basioccipital. See also Cichocki (1976: char. 6) and Kullander (1998: char. 28) for a discussion of the pharyngeal apophysis in Neotropical cichlids.

79 Expansion of the dorsal parasphenoid wing (Kullander & Nijssen 1989). [0] Absent (Fig. 5A,C); [1] present (Fig. 5B).

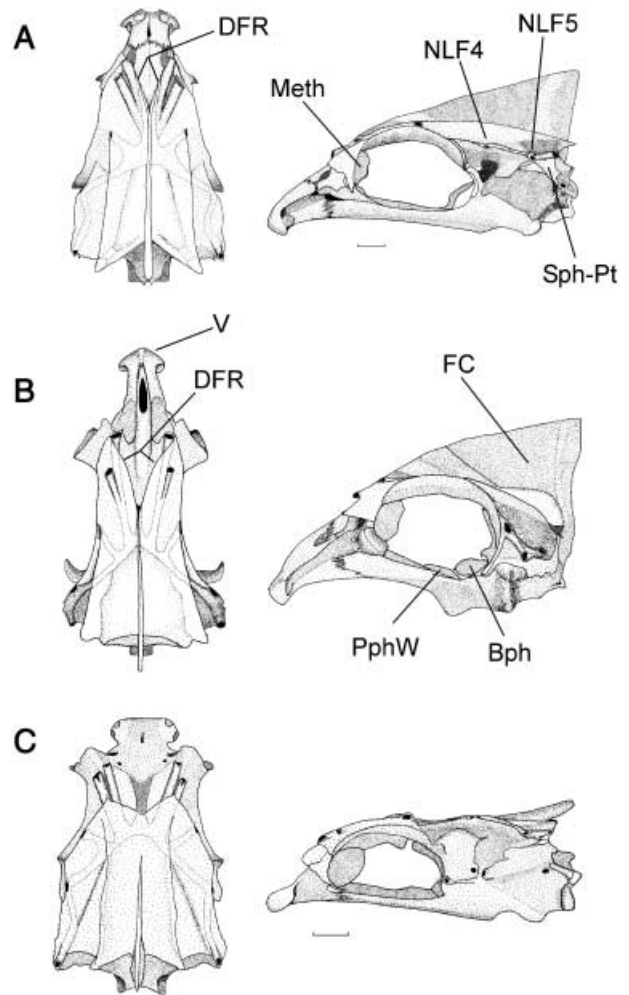


Fig. 5 A–C. Semi-diagrammatic illustration of dorsal (left) and lateral (right) view of the neurocranium (chars. 76–77, 79–81, 83–85, 88). —A. *Cichla intermedia* (AMNH, 235133). —B. *Geophagus dicrozoster* (MCNG 40623). —C. *Crenicichla* af. *lugubris* (AMNH, 235158). Scale bar = 5 mm. *Abbreviations:* Bph, basisphenoid; DFR, divergent frontal ridges; FC, frontal crest; Meth, mesethmoid; NLF4–5, neurocranial lateral line foramina; PphW, parasphenoid wing; Sph-Pt, sphenotic-pterotic canal; V, vomerine head. See Appendix 1 for character descriptions.

Kullander & Nijssen (1989: fig. 47) indicated that an expansion in both the parasphenoid wing and the basisphenoid were synapomorphic for *Acarichthys* and *Guianacara* (see also Kullander 1998: char. 36). However, an expanded parasphenoid wing is common among geophagines, and not always associated with basisphenoid expansion (see char. 80).

80 Basisphenoid expansion. [0] Absent (Fig. 5B,C). Kullander & Nijssen (1989); [1] present (Fig. 5A).

81 Caudal expansion of the mesethmoid. [0] Absent (Fig. 5B); [1] present (Fig. 5A,C). In lateral view, the mesethmoid

covers less than 1/5 of the orbital diameter (e.g. *Retroculus*); in state 1 it can cover up to 1/4 of the total orbital diameter.

82 Sphenotic foramen and canal, borne on anterodorsal region of the expanded postorbital process of the neurocranium (Stiassny 1987: fig. 6). [0] Absent; [1] present.

83 Opening of NLF4. [0] Single pore (Fig. 5A,B); [1] 2 opposed pores at the end of the tubes formed by a broken canal.

84 Opening of NLF5. [0] Single pore (Fig. 5B,C); [1] double pore (Fig. 5A); [2] NLF5 absent. State 2 observed only in *Taeniacara candidi*.

85 Orientation of sphenotic-pterotic canal. [0] Moderately angled (140–160 °) (Fig. 5A); [1] sharply angled (120 ° or less) (fig. 5B); [2] approximately straight (180 °) (Fig. 5C).

86 Suture between the vomerine wing and the parasphenoid bar (Stiassny 1991: char. 8, fig. 1.12). [0] Interdigitating; [1] straight.

87 Mesethmoid-vomer interaction (Casciotta & Arratia 1993a: char. 2). [0] Sutured; [1] not sutured.

88 Shape of the rostral margin of the vomerine head (Stiassny 1987: char. 5, fig. 5, modified). [0] Ridged (Fig. 5B); [1] indented (Fig. 5A); [2] flat (Fig. 5C).

Suspensorium and jaws

89 Foramen on the lateral face of the ascending process of the premaxilla (Cichocki 1976: char. 15). [0] Absent; [1] present.

90 Development of the palatine dermal splint (Kullander 1998: char. 50). [0] Long, largely contiguous with the rostral edge of the ectopterygoid (Fig. 6A,D–F); [1] short, reaching ectopterygoid, but not contiguous with it (Fig. 6C); [2] absent (Fig. 6B).

91 Shape of the palatine maxillary process (Kullander 1998: char. 51). [0] Flattened dorsoventrally; [1] cylindrical.

92 Posteroventral palatine laminar expansion (Cichocki 1976: char. 20, modified). [0] Narrow, thick, and largely contiguous with the anterodorsal margin of the endopterygoid; [1] approximately triangular, with a gap between the lamina and the anterodorsal edge of the endopterygoid (Fig. 6A,C,D); [2] well developed, largely contiguous with the anterodorsal margin of the endopterygoid (Fig. 6F); [3] thin and narrow, contiguity with the endopterygoid restricted to its ventral extremity or not contacting it at all (Fig. 6E); [4] lamina absent, palatine and endopterygoid not contiguous (Fig. 6F).

93 Axial lateral palatine ridge (Cichocki 1976: char. 21, modified). [0] Present (Fig. 6A,C–F); [1] absent (Fig. 6B).

94 Form of axial lateral palatine ridge. [0] Single, reduced ridge separating the maxillary process of the palatine from its posteroventral expansion; [1] single, well developed ridge in the same position as in state 0 (Fig. 6C–E); [2] bifurcated, well developed ridge with an axial arm as in states 0 and 1, and an additional maxillary or anteriorly directed ridge following the caudo-rostral direction of the maxillary process (Fig. 6F); [3] lack of medial ridge, but presence of a reduced ridge following the contour of the maxillary process (Fig. 6A).

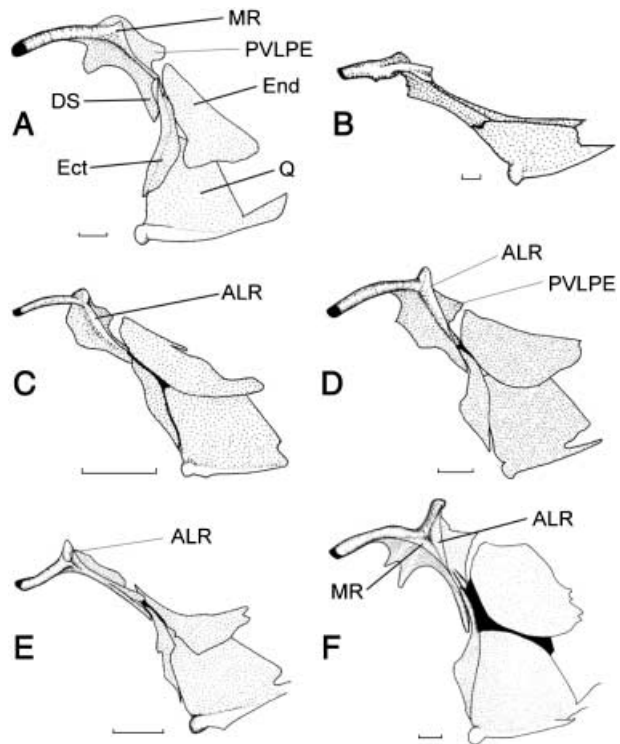


Fig. 6 A–F. Semi-diagrammatic illustration of the anterior portion of the suspensorium in left lateral view, highlighting features of the palatine and associated dermal bones (chars. 90, 92–94). —A. *Retroculus lapidifer* (MNRJ, uncatalogued). —B. *Crenicichla* af. *lugubris* (AMNH, 235158). —C. *Crenicara latruncularium* (AMNH 39751). —D. *Biotodoma cupido* (AMNH 39940). —E. *Apistogramma boignei* (MCNG, uncatalogued). —F. *Geophagus dicrozoster* (MCNG 40623). Scale bar = 1 mm. Abbreviations: ALR, axial lateral ridge of the palatine; DS, dermal splint of the palatine; Ect, ectopterygoid; End, endopterygoid; MR, maxillary ridge of the palatine; PVLPE, posteroventral laminar palatine expansion; Q, quadrate. See Appendix 1 for character descriptions.

95 Hyomandibular–metapterygoid suture (Oliver 1984: char. 24). [0] Present; [1] absent. See also Stiassny (1987: fig. 7).

96 Pointed extension of anterodorsal corner of interopercle, in medial view. [0] Absent; [1] present.

Pharyngeal osteology

97 Uncinate process of the first epibranchial relative to anterior arm (Cichocki 1976: char. 30, modified). [0] Caudally directed (Fig. 7A,B,D); [1] approximately parallel (Fig. 7C). See also Stiassny (1991: 26–27) and Kullander (1998: char. 3).

98 Relative lengths of the anterior arm and uncinat process of first epibranchial (Oliver 1984: char. 1). [0] Approximately equal (Fig. 7A,C); [1] uncinat process longer than the anterior arm (Fig. 7B,D); [2] uncinat process shorter than anterior arm. See also Oliver (1984: char. 9), Stiassny (1991:

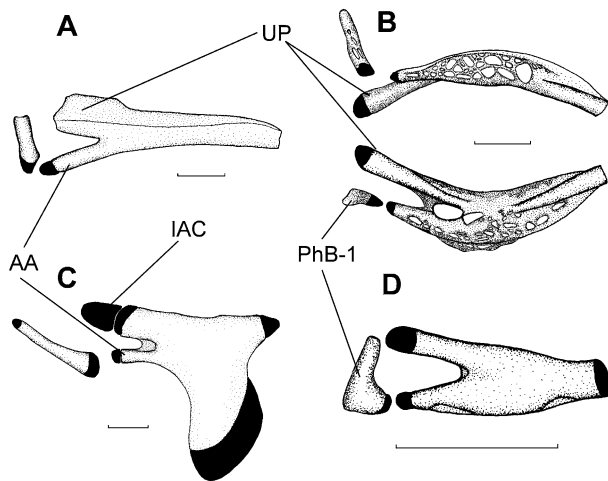


Fig. 7 A–D. Semi-diagrammatic illustration of the first epibranchial and the associated pharyngobranchial in right, approximately anterodorsal view; position of the pharyngobranchial is not necessarily natural (chars. 97–98, 100–101). —A. *Cichla temensis* (AMNH, 235139). —B. *Retroculus lapidifer* (MNRJ, uncatologued), above: approximately rostral view, below: anterodorsal view. —C. *Geophagus dicrozoster* (MCNG 40623). —D. *Crenicara latruncularium* (AMNH 39751). Scale bar = 1 mm. Abbreviations: AA, anterior arm of epibranchial 1; IAC, interarcual cartilage; PhB-1, pharyngobranchial 1; UP, uncinete process (posterior arm) of epibranchial 1. See Appendix 1 for character descriptions.

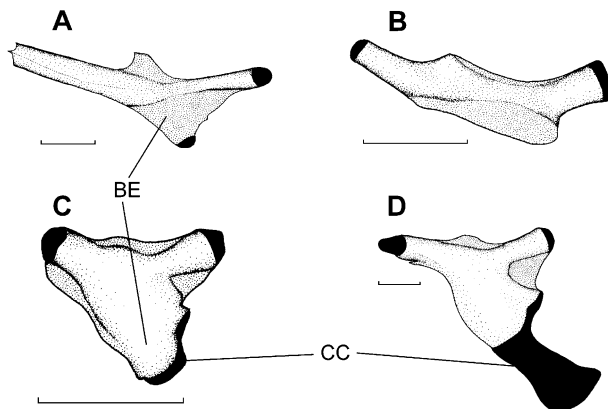


Fig. 8 A–D. Semi-diagrammatic illustration of second epibranchial in left, approximately antero-dorsal view (Character 102). —A. *Cichla temensis* (AMNH 235139). —B. *Crenicichla* af. *lugubris* (MCNG 40122). —C. *Mikrogeophagus ramirezi* (AMNH 235180). —D. *Geophagus dicrozoster* (MCNG 40623). Scale bar = 1 mm. Abbreviations: BE, bony expansion of the second epibranchial; CC, cartilage cap. See Appendix 1 for character descriptions.

char. 1, 24), and Kullander (1998: char. 1). State 2 observed only in *Cichlasoma orinocense*.

99 Deep indentation in the dorsal margin of the uncinete process of the first epibranchial (Kullander 1998: char. 3). [0] Absent;

[1] present. Mentioned by Kullander (1998: char. 3, special condition of state 2) for *Satanoperca*, but without a detailed description. We interpreted a fold, forming a sharp angle at the base of the uncinete process, as the indentation referred to by Kullander.

100 Relative widths of the uncinete process and anterior arm of epibranchial 1 (Kullander 1998: char. 4). [0] Uncinete process wider (Fig. 7A,C); [1] both processes approximately equal (Fig. 7B,D). See Kullander (1986: figs 37 and 107).

101 Development of an anterior laminar expansion (lobe) of epibranchial 1 (Cichocki 1976: char. 32). [0] Absent (Fig. 7A); [1] present, fully developed (Fig. 7C); [2] present, reduced (Fig. 7D); [3] present, deep instead of laminar (Fig. 7B).

102 Anteroventral laminar expansion of epibranchial 2. [0] Expansion present, with reduced cartilage cap (Fig. 8C); [1] expansion present without cartilage cap (Fig. 8B); [2] expansion and cartilage reduced (Fig. 8A); [3] expansion present with fully developed, axe-shaped cartilage cap (Fig. 8D).

103 Interarcual cartilage (Kullander 1998: char. 22). [0] Present, globular; [1] present, elongate; [2] absent.

104 First pharyngobranchial. [0] Bony; [1] cartilaginous.

105 Lateral expansion at the base of pharyngobranchial 1. [0] Absent; [1] present.

106 Rostricaudal flattening of pharyngobranchial 1. [0] Absent; [1] present.

107 Gill rakers on ceratobranchials (Cichocki 1976; Stiassny 1991; Kullander 1998). [0] Present; [1] absent.

108 Epibranchial 4. [0] With large expansion, with an approximately square shape of inner half of epibranchial 4 (Fig. 9B); [1] expansion triangular; [2] expansion follows the contour of epibranchial 4 (Fig. 9A).

109 Fourth ceratobranchial toothplates (Cichocki 1976: char. 39). [0] Absent; [1] present, separated from the outer gill rakers. See also Stiassny (1991: char. 3).

110 Unicuspid teeth on external gill rakers of ceratobranchial 4. [0] Present; [1] absent.

111 Lateral gill rakers on ceratobranchial 5 (Cichocki 1976: char. 40, fig. 1.21). [0] Absent; [1] present, attenuate, ossified at least at the base and lacking teeth; [2] present, forming low, rounded, and heavily ossified tooth plates.

112 Suture of the lower pharyngeal jaws (Casciotta & Arratia 1993a: char. 16). [0] Fully sutured along sagittal axis; [1] not fully sutured. Kullander (1998) indicates that this character may change ontogenetically.

113 Number of concavities in the frayed zone at the caudal edge of the fourth upper pharyngeal toothplate (Casciotta & Arratia 1993a: char. 17, fig. 24A,B). [0] 3 or more; [1] 2; [2] 1. See also Casciotta & Arratia (1993b, figs 12, 13).

Pectoral girdle

114 Anteriorly directed spinous process on the distal postcleithrum (Stiassny 1987: char. 3, fig. 2). [0] Absent; [1] present; [2]

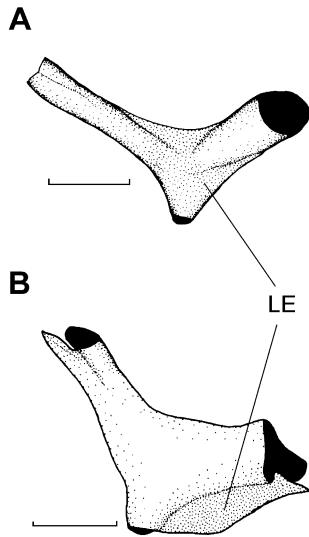


Fig. 9 A, B. Semi-diagrammatic illustration of fourth epibranchial in left, approximately anterodorsal view (char. 108). —A. *Cichla temensis* (AMNH 235139). —B. *Geophagus dicrozoster* (MCNG 40623). Scale bar = 1 mm. *Abbreviations:* LE, laminar expansion of the fourth epibranchial. See Appendix 1 for character descriptions.

present, reduced to short, blunt process directed anteriorly. Kullander (1998: char. 49) added state 2.

115 *Relative length of the medial process of the proximal extrascapula.* [0] About twice that of distal process (Fig. 10A); [1] of approximately equal length as the distal process (Fig. 10B); [2] at least 4.5–5.0 times that of distal process (Fig. 10C).

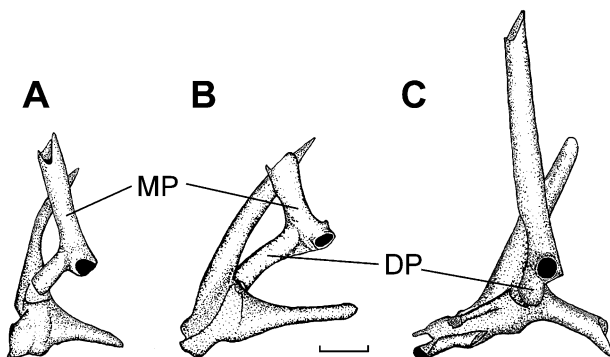


Fig. 10 A–C. Semi-diagrammatic illustration of the post-temporal and proximal extrascapula in left, lateral view (char. 115). —A. *Retroculus lapidifer* (MNRJ, uncatálogued). —B. *Cichla temensis* (AMNH 235139). —C. *Satanoperca mapiritensis* (MCNG 37262). Scale bar = 1 mm. *Abbreviations:* DP, distal process of the medial extrascapula; MP, medial process of the medial extrascapula; Ptt, post-temporal. See Appendix 1 for character descriptions.

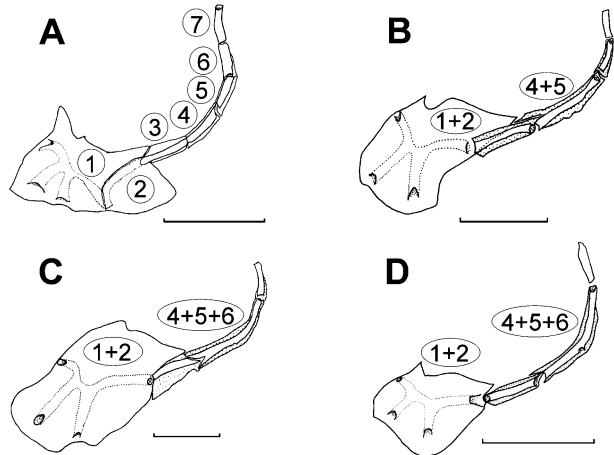


Fig. 11 A–D. Semi-diagrammatic illustration of infraorbital series in left, lateral view (chars 116–117, 119–122, 124–126). —A. *Cichla temensis* (AMNH 235139). —B. *Geophagus dicrozoster* (MCNG 40623). —C. *Satanoperca mapiritensis* (MCNG 37262). —D. *Biotodoma cupido* (AMNH 39940). Scale bar = 5 mm. *Nomenclature:* 1–7, plesiomorphic number of infraorbital ossicles, where 1 and 2 are separate lachrymals, and 7 is the dermosphenotic; 1 + 2, derived, ‘fused’ lachrymals; 4 + 5, fusion of ossicles 4 and 5; 4 + 5 + 6, fusion of ossicles 4, 5, and 6. See Appendix 1 for character descriptions and for a detailed explanation and justification of nomenclature of infraorbital bones.

Infraorbital series

Nomenclature used to name elements of the infraorbital series is generally not comparable among the work of different authors and many problems remain reconciling the differing schemes (Stiassny 1991). Here we adopt the nomenclature used by Kullander (1986). The plesiomorphic condition among Neotropical cichlids is interpreted as seven infraorbitals, including two plate-like lachrymal ossicles, as in *Cichla*, *Astronotus*, and *Retroculus* (e.g. see Kullander 1998; Farias *et al.* 1999, 2000, 2001). Nomenclature for individual ossicles is as follows (and see Fig. 11A): 1 = anteriormost lachrymal, 2 = second lachrymal (1 + 2) = the fused lachrymals, 3–6 = infraorbitals beyond lachrymal, 7 = dermosphenotic. Any combination of numbers in parentheses indicates hypothesized fusion of the corresponding elements (Fig. 11B–D). The following infraorbital characters are derived and modified from Cichocki (1976: chars. 45, 46 and 48, figs 1.24, 1.26), Oliver (1984: char.17, fig. 5), and Kullander (1998: char. 3). See also Kullander (1986; fig. 102) and Kullander (1996: fig. 13A–C).

116 *Infraorbitals 4, 5 and 6.* [0] Autogenous (Fig. 11A); [1] (4 + 5) (Fig. 11B), 6; [2] (4 + 5 + 6) (Fig. 11C,D).

117 *Lachrymals.* [0] Autogenous (Fig. 11A); [1] fused (Fig. 11B–D).

118 *Infraorbital 3.* [0] Present; [1] absent.

119 *Number of canals in lachrymal/s.* [0] 3 + 1 (three on 1, one shared by 1 and 2) (Fig. 11A); [1] 4 (Fig. 11B–D); [2] 3, this state observed only in *Biotococcus dicentrarchus*.

120 *Direction of the posterior canal of lachrymal.* [0] Posteroventral (Fig. 11A); [1] posterodorsal (Fig. 11B–D).

121 *Posterior canal of lachrymal.* [0] Open along the caudal margin, forming an open channel (Fig. 11A); [1] canal terminates in a single pore (Fig. 11B–D).

122 *Ratio of depth to length of lachrymal.* [0] Longer than deep (Fig. 11A); [1] deeper than long (Fig. 11B,C); [2] approximately as long as deep (Fig. 11D).

123 *Notch in anterodorsal edge of lachrymal.* [0] Present (Fig. 11A–D); [1] absent. See also Oliver (1984: fig. 5) and Cichocki (1976: fig. 1.24).

124 *Shape of infraorbital 3.* [0] Tubular; [1] tubular, with a ventrally directed laminar expansion (Fig. 11B–C); [2] tubular, with ventral and dorsally directed laminar expansions (Fig. 11A,D).

125 *Association between lachrymal (1 + 2 or 2) and infraorbital 3.* [0] Contiguous, but not overlapping (Fig. 11D); [1] overlapping (Fig. 11A–C).

126 *Pointed dorso-caudal laminar expansion of the lachrymal contiguous with the anterodorsal edge of infraorbital 3.* [0] Absent (Fig. 11A); [1] present (Fig. 11B–D).

Axial skeleton

127 *Supraneural bones* (predorsal bones of Cichocki 1976: char. 50). [0] 2; [1] 1; [2] 0. See also Stiassny (1991: char. 25) and Kullander (1998: char. 67).

128 *Procurrent spinous process on anterodorsal margin of first dorsal fin pterygiophore* (Cichocki 1976: char. 51). [0] Absent; [1] present.

129 *Total vertebral number* (Cichocki 1976: char. 57, modified). [0] 32 or more; [1] 26–29; [2] 23–24. See also Stiassny (1987: char. 4).

130 *Number of precaudal vertebrae* (Cichocki 1976: char. 57, modified). [0] 10–15; [1] 18–24.

131 *Number of precaudal vertebrae with centra exhibiting frontal compression* (Cichocki 1976: char. 58). [0] 3; [1] 4; [2] 2; [3] 1; [4] 0.

132 *Parhypurapophysis* (Cichocki 1976: char. 60). [0] Well developed, terminating at mid-longitudinal axis of the vertebrae; [1] absent; [2] reduced, terminating not more than one half the distance from base to mid-vertebral axis.

133 *Number of epibemal caudal ribs* (Kullander 1998: char. 75). [0] 0; [1] 7 or more.

134 *Development of vertebral hypapophyses* (Pellegrin 1904: fig. 8). [0] Short, paired; [1] long, co-ossified distally; [2] absent. See also Kullander (1998: char. 77).

135 *Vertebrae bearing expanded hypapophyses* (Pellegrin 1904). [0] 4; [1] 3.

136 *Parapophyses of first two caudal vertebrae fused, and in turn fused to first anal pterygiophore.* [0] Absent; [1] present.

Appendix 2

Material examined

Material examined in morphological analysis and voucher specimens for tissue samples used for DNA sequencing. For

each genus, the following information is given: species name, museum acronym and catalogue number; collection year; preparation and number of exemplars (A = alcohol, CS = cleared and stained, DS = dry skeleton, numbers in parentheses indicate number of vouchers from which tissue samples were taken); country of collection, drainage or state/county, collection locality. Catalogue numbers starting with an H are cross-referenced with museum numbers, indicating samples used for DNA sequencing from the tissue collection, Laboratory of Wildlife Genetics, Department of Wildlife and Fisheries Sciences, Texas A&M University. Museum abbreviations: AMNH, American Museum of Natural History, New York, USA; BM (NH), British Museum (Natural History), London, UK; MCNG, Museo de Ciencias Naturales de Guanare, Guanare, Venezuela; MNHN, Muséum National d'Histoire Naturelle, Paris, France; MNRJ, Museu Nacional do Rio de Janeiro, Brazil; NLU, North-eastern Louisiana University, Monroe, USA; TCWC, Texas Cooperative Wildlife Collection, College Station, USA. Detailed locality data, if available, can be found at the Neodat project's website (www.neodat.org) and on the websites of each museum.

Outgroup taxa

Astronotus crassipinnis: (AMNH 221982); 1987; A = 1, CS = 1; Argentina, no data. — *Astronotus* sp. (TCWC 7502.28); 1993; A = 1; Venezuela, Portuguesa, Caño Maraca at Finca Urriola. — (AMNH 235132, H6297-6298); 2001; A = 2(2); Aquarium trade. — *Cicbla intermedia*: (AMNH 235133); 2002; DS = 1; Venezuela, Apure, R Cinaruco, Pica Raya reef. — (AMNH 235134); 2002; DS = 1; Venezuela, Apure, R Cinaruco. — (AMNH 235135); 2001; A = 1; Venezuela, Apure, R Cinaruco. — (MCNG 39581); 1999; CS = 1; Venezuela, Apure, R Cinaruco. — (MCNG 41117); 1999; CS = 1; Venezuela, Apure, R Cinaruco. — (H6238, No voucher); 2000; Venezuela, Apure, R Cinaruco at Payara hole (reef point). — *Cicbla orinocensis*: (AMNH 235136); 2002; DS = 1; Venezuela, Apure, R Cinaruco, Laguna Larga N shore. — (AMNH 235137); 2002; DS = 1; Venezuela, Apure, R Cinaruco. — (TCWC 8312.08); 1994; A = 2, CS = 3; Venezuela, Bolívar, R Caroní, NE Guri reservoir near dam F. — (TCWC 7500.37); 2001; A = 1; Venezuela, Apure, R Cinaruco at Laguna Larga. — (H6237, No voucher); 2000; Venezuela, Apure, R Cinaruco at Payara hole (reef point). — *Cicbla temensis*: (AMNH 235138); 2002; DS = 1; Venezuela, Apure, R Cinaruco, Laguna Larga. — (AMNH 235139); 1994; A = 7, CS = 3; Venezuela, Apure, R Cinaruco. — (AMNH Uncatalogued) 2000; A = 1; Venezuela, Apure, R Cinaruco, Laguna Larga at mouth of Caño Largo. — (AMNH 235140); 2000; A = 1; Venezuela, Apure, R Cinaruco at Laguna Larga. — (H6239, No voucher); 2000; Venezuela, Apure, R Cinaruco at Payara hole (reef point). *Cicbla ocellaris*: (AMNH 97396); No date; CS = 1; No data. — *Retroculus lapidifer*: (BM (NH) 1970.10.28 : 59);

1968; A = 1; Brazil, Mattogrosso, Rio das Mortes, Xaventina Island. — (MNRJ Uncatalogued) 1999; A = 3, CS = 2; Brazil, Goiás, R Maranhão, Cachoeria do Macadinho. — (MNRJ SM 21–521 E. P. Caramaschi) 1999; A = 1; Brazil, Rio Tocantins, Serra da Mesa reservoir dam. — *Retroculus* sp. (H6293, No known voucher); No date; Brazil, Macapá.

Ciclasomatinae

Ciclasoma orinocense: (AMNH 235141, H6209–6210); 2000; CS, T = 2; Venezuela, Apure, road from La Pedrera (Táchira State) to Guasualito, few minutes after Las Guacas. — (AMNH 235142, H6211); 2000; A = 2(2); Venezuela, Apure, Caño Maporal iron bridge, road to UNELLEZ modulo. — *Hoplarchus psittacus*: (AMNH 235143); 2002; DS = 1; Venezuela, Apure, R Cinaruco. — (AMNH 235144); 2002; DS = 1; Venezuela, Apure, R Cinaruco. — (MCNG 39961); 1999; A = 7, CS = 2; Venezuela, Apure, R Cinaruco, Laguna Oheros. — (MCNG uncatalogued, H6241); 2000; A = 1(1); Venezuela, Apure, R Cinaruco, Caño mouth of Laguna Larga. — *Mesonauta egypticus*: (AMNH 235145, H6226–6227); 2000; A = 3(3), CS = 1(1); Venezuela, Apure, Caño Maporal iron bridge, road to UNELLEZ modulo. *Ciclasomatinae*. *Heros* n. sp. ‘common’ (AMNH 235192); 2002; DS = 1; Venezuela, Apure, R Cinaruco. — (AMNH 235193); 2002; DS = 1; Venezuela, Apure, R Cinaruco. — *Mesonauta festivum*: (AMNH 40053); 1964; CS = 3; Bolivia, Beni, R Baures, 500 miles above mouth, on left.

Geophaginae

Acaricthys heckelii: (AMNH 14352); 1937; A = 3, CS = 2; Guyana, Essequibo, Essequibo R Rockstone. — (AMNH 221358); 1977; A = 1; Brazil, Amazonas, branch of the R Janauacá mouth of Lago do Castanho. — (AMNH 235146, H6288–6289); 2000; A = 2(2); Aquarium trade. — *Apistogrammoides pucallpaensis*: (AMNH 235147, H6203–6204); 1999; A = 8(4), CS = 2; Perú, R Orosa, Pacaurillo and/or Madre Selva reserve. — *Apistogramma boignei*: (AMNH 235148); 2000; A = 1; Venezuela, Apure, road from La Pedrera (Táchira State) to Guasualito, a few minutes after Las Guacas. — (AMNH 235149, H6223); 2000; A = 4(3); Venezuela, Apure, Caño Maporal iron bridge on the road to UNELLEZ modulo. — *Apistogramma agassizi*: (AMNH 21582); No date; CS = 1; Perú, Amazon basin. — (AMNH 235150, H6199–6200); 1999; A = 3(3); Perú, R Orosa, Pacaurillo and/or Madre Selva reserve. — *Biotodoma cupido*: (AMNH 40148); 1964; A = 1; Bolivia, Beni, Arroyo Grande, 2 km W Guayamerín, c. 1.5 km above mouth. — (AMNH 215177); No date; A = 47; Guyana, Demerara, Malali. — (AMNH 39940); 1964; A = 10, CS = 2; Bolivia, Beni, R Iténez, 2 km SE Costa Marques, Brazil. — (AMNH 43359); 1935; CS = 1; Guyana, Demerara, Malali. — (AMNH Uncatalogued; H6195–6196); 1999; A = 3, T = 3; Perú, R Orosa, Pacaurillo reserve. — *Biotodoma wavrini*: (AMNH 235151); 1999; A = 17, CS = 2; Venezuela, Apure, R Cinaruco Laguna Larga. — (MCNG 41367, H6202); 1999; A = 1(1);

Venezuela, Apure, R Cinaruco Laguna Larga. — (AMNH 235152, H6230); 2000, A = 6(6); Venezuela, Apure, R Cinaruco Payara hole (reef point). — (AMNH 235153); 2000, A = 2; Venezuela, Apure, R Cinaruco, Laguna Larga mouth of Caño Largo. — *Biotocetus dicentrarchus*: (AMNH 221350); 1977; A = 1; Brazil, Amazonas, Ilha de Marchantaria. — (NLU 75944); 1999; A = 20; Venezuela, Apure, R Cinaruco Laguna Larga. — (AMNH 235154); 1999; A = 1; Venezuela, Apure, R Cinaruco. — (AMNH 235155, H6249–6250); 2000; A = 12(6), CS = 4; Venezuela, Apure, R Cinaruco Laguna Larga. — *Crenicara punctulatum*: (AMNH 78126); 1987; A = 1; Perú, Loreto, R Tahuayo, tributary of R Amazonas, Huasi village. — (AMNH 39917); 1964; CS = 2; Bolivia, Beni, Pond in arroyo below lower campo of Pampa de Meio, c. 12 km SE Costa Marques, Brazil. — *Crenicara latruncularium*: (AMNH 39751); 1964; A = 13, CS = 2; Bolivia, Beni, R Iténez, 2 km SE Costa Marques, Brazil. — (AMNH 235156, H6301–6302); 2003; A = 2(2); Aquarium trade. — *Crenicichla geayi*: (AMNH 235157, H6207–6208); 2000; A = 1(1) CS = 1(1); Venezuela, Portuguesa, R Las Marías Quebrada Seca. — *Crenicichla* af. *lugubris*: (AMNH 235158); 2002; DS = 1; Venezuela, Apure, R Cinaruco, Caño Largo. — (AMNH 235159); 2002; DS = 1; Venezuela, Apure, R Cinaruco. — (AMNH 235160); 2002; DS = 1; Venezuela, Apure, R Cinaruco. — (MCNG 40225); 1999; A = 1; Venezuela, Apure, R Cinaruco Laguna Larga. — (MCNG 41034); 1999; A = 1; Venezuela, Apure, R Cinaruco Laguna Estrechura. — (MCNG 40122); 1999; CS = 1; Venezuela, Apure, R Cinaruco Laguna Las Guayabas. — (H6230, No voucher); 2000; Venezuela, Apure, R Cinaruco Payara hole (reef point). — (H6242, No voucher); 2000; Venezuela, Apure, R Cinaruco Laguna Larga. — *Crenicichla sveni*: (AMNH 235161, H6213–6214); 2000; A = 2(2) CS = 2(2); Venezuela, Apure, road between Guasualito and Elorza. — *Crenicichla* af. *wallacii*: (AMNH 235162, H6244–6245); 2000; A = 2(2), CS = 2(2); Venezuela, Apure, R Cinaruco Laguna Larga. — (AMNH 235163); 2000; A = 2; Venezuela, Apure, R Cinaruco, Laguna Larga mouth of Caño Largo. — *Dicrosus filamentosus*: (MCNG 12190); 1985; A = 12, CS = 5; Venezuela, Amazonas, Caño Iguarapo, aprox. 1 km above mouth, near Piedra de Culimacare of R Casiquiare. — *Dicrosus* sp. (H6285, Sample is voucher); 2000; Aquarium trade. — *Geophagus abalios*: (AMNH 235164); 2002; DS = 1; Venezuela, Apure, R Cinaruco. — (AMNH 235165); 2002; DS = 1; Venezuela, Apure, R Cinaruco. — (MCNG 40636); 1999; CS = 1; Venezuela, Apure, R Cinaruco. — (H6259–6260, No vouchers); 2000; Venezuela, Apure, R Cinaruco Laguna Larga. — *Geophagus brachybranchus*: (AMNH 72130); 1982; A = 2; Guyana, Essequibo, sandbar on N bank of Cuyun’ R, just W of Caowrie creek mouth. — (AMNH 215202); No date; A = 19; Guyana, Demerara, Demerara R Wismar. — (AMNH 72098); 1982; A = 2; Guyana, Essequibo, Kartabo point, between Cuyuní R mouth and Mazaruni river mouth. — (AMNH 54944); 1979; CS = 3; Surinam, Nickerie, Camp Hydro, c. km 370, c. 30 km N Tiger Falls. —

- (AMNH 54881); 1979; A = 26; Surinam, Nickerie, Toeboeroe creek, km 220, 300–900 m from mouth. — (AMNH 235166, H6271-6272); 2000; A = 3(3); Surinam, Nickerie, Toeboeroe creek, km 220, 300–900 m from mouth. — *Geophagus dicrozoster*: (AMNH 235167); 2002; DS = 1; Venezuela, Apure, R Cinaruco, Caño Largo. — (AMNH 235168); 2002; DS = 1; Venezuela, Apure, R Cinaruco. — (AMNH 235169, H6255-6256); 2000; A = 5(4); Venezuela, Apure, R Cinaruco Laguna Larga. — (AMNH 235170); 2000; A = 1; Venezuela, Apure, R Cinaruco Payara hole (reef point). — *Geophagus grammepareius*: (MCNG 34396); 1994; A = 2, CS = 3; Venezuela, Bolívar, R Caroní near R Claro. — (AMNH 235171, H6265); 2000; A = 1: 1; Venezuela, Bolívar, R Claro bridge on the road to Guri. — *Geophagus surinamensis*: (MNHN 2001.2275); 2001; A = 2; French Guiana, Antécume Pata, Upper Maroni R. — (MNHN 2001.2279, H6299); 2001; A = 2(1); French Guiana, Antécume Pata, Upper Maroni R. — (MNHN 2001.2280, H6300); 2001; A = 2(1); French Guiana, Antécume Pata, Upper Maroni R. — (MNHN 2001.2281); 2001; A = 3, CS = 2; French Guiana, Antécume Pata, Upper Maroni R. — '*Geophagus*' *brasiliensis*: (AMNH 222386); 1991; A = 7, CS = 3; Brazil, São Paulo, R Pardo Riberão Preto. — (AMNH 235172, H6286-6287); 2000; A = 2(2); Aquarium trade. — '*Geophagus*' *steindachneri*: (MCNG 758); 1976; A = 11, CS = 2; Venezuela, Trujillo, R Motatán Puente 3 de febrero. — (AMNH 235173, H6283-6284); 2001; A = 2: 2; Aquarium trade. — *Guianacara* n. sp. 'caroni': (AMNH 91068); 1990; CS = 1; Venezuela, Bolívar, R Paragua above second rapids above R Carapo mouth. — (AMNH 235174, H6266-6267); 2000; A = 27(5), CS = 2; Venezuela, Bolívar, R Claro, bridge on the way to Guri. — *Gymnogeophagus balzanii*: (AMNH 1278); 1901; A = 1, CS = 1; Paraguay, R Paraguay Asunción. — (AMNH 235175, H6296); 2001; Aquarium trade. — *Gymnogeophagus rhabdotus*: (AMNH 235176, H6297); 2001; A = 1: 1. Aquarium trade. — (AMNH 12348); 1933; A = 5, CS = 3; Argentina, Buenos Aires. — (AMNH 235177, H6294-6295); 2001; A = 2(2). Aquarium trade. — *Mikrogeophagus altispinosus*: (AMNH 235178, H6278-6279); 2000; A = 5(5), CS = 2; Aquarium trade. — *Mikrogeophagus ramirezi*: (AMNH 235179); 2000; A = 1; Venezuela, probably Monagas State, no other data available. — (AMNH 235180, H6217-6218); 2000; A = 4(4), CS = 2(2); Venezuela, Apure, Caño Maporal iron bridge on the way to UNELLEZ modulo. — *Satanoperca daemon*: (AMNH 235181); 2002; DS = 1; Venezuela, Apure, R Cinaruco. — (AMNH 235182); 2002; DS = 1; Venezuela, Apure, R Cinaruco. — (AMNH 235183); 2002; DS = 1; Venezuela, Apure, R Cinaruco. — (AMNH 235184); 2000; A = 5; Venezuela, Apure, R Cinaruco, Laguna Larga mouth of Caño Largo. — (AMNH 235185); 1999; A = 6, CS = 1; Venezuela, Apure, R Cinaruco Laguna Larga. — (MCNG 37255); 1997; A = 1, CS = 1; Venezuela, Guárico, Aguaro-Guariquito National Park, Caño char.arcotico. — (AMNH 235186, H6261-6261); 2000; A = 2: 2; Venezuela, Apure, R Cinaruco Laguna Larga. — (MCNG Uncatalogued, H6248); 2000; A = 1(1); Venezuela, Apure, R Cinaruco Laguna Larga. — *Satanoperca jurupari*: (AMNH 12752); 1934; A = 8, CS = 1; Brazil, Amazonas, R Livramento, tributary of R Madeira. — (AMNH 235187, H6198); 1999; A = 1(1); Perú, R Orosa Yanashi. — (H6198, No voucher); 1999; Perú, Caño Santa Rita, Nanay drainage. — *Satanoperca mapiritensis*: (AMNH 235188, H6263-6264); 2000; A = 2(2); Venezuela, Bolívar, R Pao the most E cross with road between Maripa and Ciudad Bolívar. — (AMNH 235189, H6274-6275); 2000; A = 4(4); Venezuela, Anzoátegui, R Morichal Largo. — (AMNH 235190); 1999; CS = 1; Venezuela, Apure, R Cinaruco Laguna Larga. — *Satanoperca pappaterra*: (AMNH 40103); 1964; A = 8, CS = 2; Brazil, Rondonia, Overflow pond of R Guaporé 1 km W Costa Marques. (H6309-6310, No vouchers); 2000; Brazil, R Paraná. — *Taeniacara candidi*: (AMNH 235191, H6290-6291); 2000; A = 2(2), CS = 1; Aquarium trade. *Biotodoma* af. *cupido*: (AMNH 12751); 1934; A = 2; Brazil, Amazonas, R Livramento, tributary of R Madeira. — *Guianacara sphenozona*: (AMNH 54857); 1979; A = 5; Surinam, Nickerie, Kabelebo R, 1 km S Avanavero falls. — (AMNH 54763); 1979; A = 18; Surinam, Nickerie, Kapoeri creek, c. 7 km from junction of Corintijn [Corantijn] R. — (AMNH 17635); 1938; A = 4; Guyana, Essequibo, blackwater creek Essequibo R headwaters. — (AMNH 54939); 1979; CS = 5; Surinam, Nickerie, Camp Hydro, c. km 370, c. 30 km N Tiger Falls. — *Gymnogeophagus gymno-genys*: (AMNH 57055); 1985; A = 2, CS = 1; Brazil, R Grande do Sul, near Porto Alegre. — *Geophagus harreri*: (AMNH 16434); 1939; A = 2; Surinam, Marowijne, Litani R near Tapoute. — *Geophagus megasema*: (AMNH 39936); 1964; A = 1; Bolivia, Beni, R Iténez 5 km SW Costa Marques, Brazil. — *Geophagus taeniopareius*: (AMNH 56180); 1981; A = 2, CS = 2; Venezuela, Amazonas, R Cataniapo, c. 800 m from mouth, near Puerto Ayacucho. — *Satanoperca leucosticta*: (AMNH 215096); 1935; A = 8; Guyana, Demerara, Demerara R Wismar. — (AMNH 7090); 1908; A = 3; Guyana, Demerara, Maduni creek. — (AMNH 214849); 1934; A = 2; Guyana, Demerara, Demerara R Malali. — (AMNH 215206); No date; Guyana, Demerara, Demerara R Wismar.
- African taxa*
Serranochromis mellandi: (AMNH 9011); 1925; A = 4; Angola, Cunene R Capelongo. — *Paratilapia polleii*: (AMNH 217760); 1988 or 1990; CS = 1; No data. — *Ptychochromis oligacanthus*: (AMNH 97028); 1990; A = 3, CS = 2; Madagascar, Tamatave, Bay Lake, 1 km S of turnoff from Marolambo-Mananjary road. — *Ptychochromoides katria*: (AMNH 93700); 1990; CS = 5; Madagascar, R Novosivolo below Zule's village, large side-pool off mainstream. — *Tylochromis leonensis*: (AMNH 59650); 1990; A = 11; Sierra Leone, R Taia, Taiama Bridge. — *Tylochromis variabilis*: (AMNH 57162); 1915; CS = 1; Congo, Stanleyville.

Continued

	1111111111111111
	222222223333333
	1234567890123456
<i>Acarichthys heckelii</i>	110?111010000010
<i>Apistogramma agassizi</i>	10101110202102-0
<i>Apistogramma hoignei</i>	?0?01?10202102-0
<i>Apistogrammoides pucallpaensis</i>	10111110202102-0
<i>Astronotus</i> sp.	100000000010100
<i>Biotodoma cupido</i>	1202010010000010
<i>Biotodoma wavrini</i>	1202010010000010
<i>Biotoecus dicentrarchus</i>	?00--01010220010
<i>Cichla intermedia</i>	0002100000200010
<i>Cichla orinocensis</i>	0002100000200010
<i>Cichla temensis</i>	0002100000200010
<i>Cichlasoma orinocense</i>	1010100010120000
<i>Crenicara punctulatum</i>	1000001010020010
<i>Crenicichla geayi</i>	?00???20014102-0
<i>Crenicichla af. lugubris</i>	10001020012102-0
<i>Crenicichla sveni</i>	?0?0?020013102-0
<i>Crenicichla af. wallacei</i>	?000?020013102-0
<i>Dicrosus</i> sp.	10000110102202-0
<i>Geophagus abalios</i>	1101111010001110
	1111111111111111
	222222223333333
	1234567890123456
<i>Geophagus brachybranchus</i>	1101111010001110
<i>Geophagus dicrozoster</i>	1101111010001110
<i>Geophagus grammepareius</i>	1101111010001110
<i>Geophagus surinamensis</i>	1101111010001110
' <i>Geophagus</i> ' <i>brasiliensis</i>	?200011010220010
' <i>Geophagus</i> ' <i>steindachneri</i>	1101111010200110
<i>Guianacara</i> n. sp. 'caroni'	1102110010000010
<i>Gymnogeophagus balzanii</i>	1101112110000110
<i>Gymnogeophagus rhabdotus</i>	1201112110020110
<i>Hoplarchus psittacus</i>	1200100010020111
<i>Mesonauta egregius</i>	1200100010010111
<i>Mikrogeophagus altispinosus</i>	1002101010020010
<i>Mikrogeophagus ramirezi</i>	1000001010020010
<i>Retroculus</i> sp.	0101010000000000
<i>Satanoperca daemon</i>	1100111010100110
<i>Satanoperca jurupari</i>	1101111010100110
<i>Satanoperca mapiritensis</i>	1101111010100110
<i>Satanoperca pappaterra</i>	110?111010100110
<i>Taeniacara candidi</i>	?00--010202102-0